



VEHICULAR 2012

The First International Conference on Advances in Vehicular Systems,
Technologies and Applications

ISBN: 978-1-61208-241-7

June 24-29, 2012

Venice, Italy

VEHICULAR 2012 Editors

Eugen Borcoci, University 'Politehnica' of Bucharest, Romania

Pascal Lorenz, University of Haute Alsace, France

Petre Dini, Concordia University, Canada / China Space Agency Center, China

VEHICULAR 2012

Foreword

The First International Conference on Advances in Vehicular Systems, Technologies and Applications [VEHICULAR 2012], held between June 24-29, 2012 - Venice, Italy, was an inaugural event considering the state-of-the-art technologies for information dissemination in vehicle-to-vehicle and vehicle-to-infrastructure and focusing on advances in vehicular systems, technologies and applications.

Mobility brought new dimensions to communication and networking systems, making possible new applications and services in vehicular systems. Wireless networking and communication between vehicles and with infrastructure have specific characteristics from other conventional wireless networking systems and applications (rapidly-changing topology, specific road direction of vehicle movements, etc.). These led to specific constraints and optimizations techniques; for example, power efficiency is not as important for vehicle communications as it is for traditional ad hoc networking. Additionally, vehicle applications demand strict communications performance requirements that are not present in conventional wireless networks. Services can range from time-critical safety services, traffic management, to infotainment and local advertising services. They are introducing critical and subliminal information. Subliminally delivered information, unobtrusive techniques for driver's state detection, and mitigation or regulation interfaces enlarge the spectrum of challenges in vehicular systems.

We take here the opportunity to warmly thank all the members of the VEHICULAR 2012 Technical Program Committee, as well as the numerous reviewers. The creation of such a high quality conference program would not have been possible without their involvement. We also kindly thank all the authors who dedicated much of their time and efforts to contribute to VEHICULAR 2012. We truly believe that, thanks to all these efforts, the final conference program consisted of top quality contributions.

Also, this event could not have been a reality without the support of many individuals, organizations, and sponsors. We are grateful to the members of the VEHICULAR 2012 organizing committee for their help in handling the logistics and for their work to make this professional meeting a success.

We hope that VEHICULAR 2012 was a successful international forum for the exchange of ideas and results between academia and industry and for the promotion of progress in the field of vehicular systems, technologies and applications.

We are convinced that the participants found the event useful and communications very open. We also hope the attendees enjoyed the charm of Venice, Italy.

VEHICULAR 2012 Chairs:

Eugen Borcoci, University 'Politehnica' of Bucharest, Romania

Pascal Lorenz, University of Haute Alsace, France

Petre Dini, Concordia University, Canada / China Space Agency Center, China

VEHICULAR 2012

Committee

VEHICULAR Advisory Committee

Eugen Borcoci, University 'Politehnica' of Bucharest, Romania
Pascal Lorenz, University of Haute Alsace, France
Petre Dini, Concordia University, Canada / China Space Agency Center, China

VEHICULAR Technical Program Committee

Aydin Akan, Istanbul University, Turkey
Waleed Alasmay, University of Toronto, Canada
Andrea Baiocchi, SAPIENZA University of Rome, Italy
Irina Balan, Ghent University - IBBT, Belgium
Monique Becker, Institut Mines Telecom, France
Luis Bernardo, Universidade Nova of Lisboa, Portugal
Yuanguo Bi, Northeastern University, China
Pascal Bodin, Orange Labs, France
Mélanie Bourouche, Trinity College Dublin, Ireland
Robert Budde, TU Dortmund University, Germany
Chiara Buratti, DEIS, University of Bologna, Italy
Maria Calderon, University Carlos III of Madrid, Spain
Jean Pierre Cances, University of Limoges, France
Hongyang Chen, Fujitsu Labs. Ltd, Japan
Lien-Wu Chen, Feng Chia University - Taichung, Taiwan
Chien-Liang Chen, Aletheia University - Taipei, Taiwan
Ray-Guang Cheng, National Taiwan University of Science and Technology - Taipei, Taiwan, R.O.C.
Yonggang Chi, Harbin Institute of Technology, China
Dong Ho Cho, Korea Advanced Institute of Science and Technology - Daejeon, Republic of Korea
Juan Antonio Cordero Fuertes, INRIA, France
Carl James Debono, University of Malta - Msida, Malta
Trung Q. Duong, Blekinge Institute of Technology, Sweden
Weiwei Fang (方维维), Beijing Jiaotong University (BJTU) - Beijing, China
Michel Ferreira, University of Porto and Instituto de Telecomunicações, Portugal
Alois Ferscha, Institut für Pervasive Computing, Johannes Kepler Universität Linz, Austria
Malgorzata Gajewska, Gdansk University of Technology, Poland
Slawomir Gajewski, Gdansk University of Technology, Poland
Hassan Ghasemzadeh, University of California - Los Angeles, USA
Athanasios Gkelias, Imperial College London, UK

Javier Gozalvez, UWICORE Laboratory, University Miguel Hernandez of Elche, Spain
An He, Qualcomm, USA
Jianhua He, Swansea University, UK
Khelifa Hettak, Industry Canada / Communications Research Centre - Nepean, Canada
Daesik Hong, Yonsei University - Seoul, Korea
Daniel Jiang, Mercedes-Benz Research & Development North America, USA
Georgios Karagiannis, University of Twente, The Netherlands
Gunes Karabulut Kurt, Istanbul Technical University - Istanbul, Turkey
John Lee, Telcordia Technologies Inc., USA
Jungwoo Lee, Seoul National University, Korea
Jingli Li, Emerson Electric Co. - Louisville, USA
XiangYang Li, Illinois Institute of Technology - Chicago, USA
Qilian Liang, University of Texas at Arlington, USA
Kuang-Hao Lin, National Chin-Yi University of Technology, Taiwan
Thomas Little, Boston University, USA
Rongxing Lu, University of Waterloo, Canada
Johan Lukkien, Eindhoven University of Technology, The Netherlands
Barbara M. Masini, CNR - IEIT, University of Bologna, Italy
Abolfazl Mehdodniya, Tohoku University, Japan
Ingrid Moerman, Ghent University - IBBT, Belgium
Hidekazu Murata, Kyoto University, Japan
Stefan Nowak, TU Dortmund University, Germany
Shumao Ou, Oxford Brookes University, UK
Mohammad Patwary, Staffordshire University, UK
Matthias Uwe Pätzold, University of Agder - Grimstad, Norway
Adrian Popescu, Blekinge Institute of Technology - Karlskrona, Sweden
Ravi Prakash, University of Texas at Dallas, USA
M. Elena Renda, IIT - CNR - Pisa, Italy
Tapani Ristaniemi, University of Jyväskylä, Finland
Marco Rocchetti, University of Bologna, Italy
Won-Yong Shin, Harvard University, USA
Marcin Sokół, Gdansk University of Technology, Poland
Hwangjun Song, POSTECH (Pohang Univ of Science and Technology) - Pohang, Korea
Kemal Ertugrul Tepe, University of Windsor, Canada
Carlo Vallati, University of Pisa, Italy
Fabrice Valois, INRIA SWING / CITI, INSA-Lyon, France
Necmi Taspinar, Erciyes University - Kayseri, Turkey
Olav Tirkkonen, Aalto University, Finland
Theodoros A. Tsiftsis, Technological Educational Institute of Lamia, Greece
Wenjing Wang, Blue Coat Systems, Inc., USA
Yue Wang, Toshiba Research Europe Ltd. - Bristol, UK
You-Chiun Wang, National Sun Yat-Sen University, Taiwan
André Weimerskirch, escrypt Inc., USA
Chih-Yu Wen, National Chung Hsing University - Taichung, Taiwan

Weidong Xiang, University of Michigan - Dearborn, USA

Zheng Yan, Aalto University - Espoo, Finland / Xidian University Xi'an, China

Wei Yuan, Huazhong University of Science and Technology - Wuhan, China

Peng Zhang, Xi`An University of Posts and Telecommunications (XUPT), China

Wensheng Zhang, Iowa State University, USA

Zhangbing Zhou, China University of Geosciences - Beijing, China & TELECOM SudParis, France

Haojin Zhu, Shanghai Jiao Tong University, China

Yanmin Zhu, Shanghai Jiao Tong University, China

Copyright Information

For your reference, this is the text governing the copyright release for material published by IARIA.

The copyright release is a transfer of publication rights, which allows IARIA and its partners to drive the dissemination of the published material. This allows IARIA to give articles increased visibility via distribution, inclusion in libraries, and arrangements for submission to indexes.

I, the undersigned, declare that the article is original, and that I represent the authors of this article in the copyright release matters. If this work has been done as work-for-hire, I have obtained all necessary clearances to execute a copyright release. I hereby irrevocably transfer exclusive copyright for this material to IARIA. I give IARIA permission to reproduce the work in any media format such as, but not limited to, print, digital, or electronic. I give IARIA permission to distribute the materials without restriction to any institutions or individuals. I give IARIA permission to submit the work for inclusion in article repositories as IARIA sees fit.

I, the undersigned, declare that to the best of my knowledge, the article does not contain libelous or otherwise unlawful contents or invading the right of privacy or infringing on a proprietary right.

Following the copyright release, any circulated version of the article must bear the copyright notice and any header and footer information that IARIA applies to the published article.

IARIA grants royalty-free permission to the authors to disseminate the work, under the above provisions, for any academic, commercial, or industrial use. IARIA grants royalty-free permission to any individuals or institutions to make the article available electronically, online, or in print.

IARIA acknowledges that rights to any algorithm, process, procedure, apparatus, or articles of manufacture remain with the authors and their employers.

I, the undersigned, understand that IARIA will not be liable, in contract, tort (including, without limitation, negligence), pre-contract or other representations (other than fraudulent misrepresentations) or otherwise in connection with the publication of my work.

Exception to the above is made for work-for-hire performed while employed by the government. In that case, copyright to the material remains with the said government. The rightful owners (authors and government entity) grant unlimited and unrestricted permission to IARIA, IARIA's contractors, and IARIA's partners to further distribute the work.

Table of Contents

Acoustic Sensor Network for Vehicle Traffic Monitoring <i>Barbara Barbagli, Gianfranco Manes, Rodolfo Facchini, and Antonio Manes</i>	1
A Prototypical In-Car Entertainment Setup Using Software Defined Radio and Ethernet/IP-Based In-Vehicle Communication <i>Lothar Stolz, Kay Weckemann, Hyung-Taek Lim, and Walter Stechele</i>	7
Model, Analysis, and Improvements for V2V Communication Based on 802.11p <i>Tseesuren Batsuuri, Reinder J. Bril, and Johan J. Lukkien</i>	11
Efficient Adaptive Equalizer Combined with LDPC Code for Vehicular Communications <i>Do-Hoon Kim, Junyeong Bok, and Heung-Gyoon Ryu</i>	18
Intelligent Traffic Control Based on Multi-armed Bandit and Wireless Scheduling Techniques <i>Chanwoo Park and Jungwoo Lee</i>	23

Acoustic Sensor Network for Vehicle Traffic Monitoring

Barbara Barbagli, Gianfranco Manes, Rodolfo Facchini
 Department of Electronics and Telecommunications, University of Florence
 Via di Santa Marta 3, 50139 Florence, Italy,
 Email: barbara.barbagli@gmail.com, gianfranco.manes@unifi.it
 rfacch@gmail.com

Antonio Manes
 Netsens S.r.l.
 Via Tevere 70, 50019 Florence, Italy
 Email: antonio.manes@netsens.it

Abstract—Real time traffic monitoring is a fundamental requirement for improving the efficiency of transportation systems. The emerging technology of wireless sensor networks (WSNs) allows of distributed traffic monitoring systems at large scale with low cost of installation and maintenance. The develop of cheap sensor nodes with integrated computing and wireless communication capabilities has changed the scenery of real-time traffic data acquisition. This paper describes a WSN based on an array of acoustic sensor employing an effective signal processing and a novel parameter estimation procedure. Key features are traffic monitoring and localization of traffic congestion event performed in real time, with an impressive space scale. A particular case study is presented starting from a real problem and achieving the best architectural solution. Finally the results of theoretical analysis and extensive experimental results of a prototype installation on a motorway are provided.

Keywords - wireless sensor networks; traffic monitoring system; acoustic sensors; vehicle detection; traffic parameters estimation.

I. INTRODUCTION

Traffic monitoring and vehicle detection is of paramount importance in Intelligent Transportation Systems (ITS). Improving the efficiency of transportation systems has tremendously economical and environmental impact. Traffic management systems, to address the task of an effective management road strategies, require accurate estimation of traffic parameters such as average vehicle speed, density, percentage of occupancy lane. A desirable traffic monitoring system should (i) allows a large-scale deployment, (ii) be passive and operate at low power, (iii) operate in all weather day-night conditions, and (iv) be cheap and easy to install and maintain.

System design must include the choice of a particular sensor as well as the development of adequate signal processing and parameters estimation method.

Many alternatives exist for collecting data about the transit of road vehicles at a given location. Traffic sensors commercially available at present can be divided into two groups, intrusive and non-intrusive sensors, based on their placement. Sensor placement has significant effects on the cost of installation and maintenance, quality of sensing, lifetime of sensors, and disruption of traffic.

Intrusive sensors include inductive loops, magnetometers, microloop probes, pneumatic road tubes, piezoelectric cables,

and other weigh-in-motion sensors. They are installed directly on the pavement surface. The main advantage of these sensors is their high accuracy for vehicle detection. However, they have some drawbacks especially the high cost due to the disruption of traffic during installation or repair. As a results, those solutions are not suitable for large-scale deployment and hence are restricted to small scale applications.

These limitations have pushed towards the development of non-intrusive traffic monitoring technologies, including radar, infrared, or ultrasound based detectors; video cameras and microphones. Like the former sensors, the latter could detect vehicle's transit and also they could provide vehicle speed, vehicle classification, and lane coverage. On the other hand, they are expensive, power-hungry and may be affected by different environmental conditions.

The acoustic sensors are attractive especially for the low cost for unit and the simple and non intrusive installation, but at the same time they require sophisticated post-processing algorithm to extract useful information. The problem of detecting vehicles with passive acoustic transducer has been addressed in many studies. Mainly, two approach have been developed: with a single transducer or with an array of microphones. In particular Lo and Ferguson [5] have formulated a nonlinear least-squares method to estimate the motion parameters of a target with broadband acoustic energy spectrum. Valcarce et al. [4] have proposed a maximum likelihood estimate for vehicle speed detection. Forren and Jaarsma [2] have detected vehicles by exploiting the tire noise, using signal correlations among three known microphones under assumption that vehicle has signal with a stationary characteristic. However, they do not model any interference effects of the tires.

Another relevant requirement pushing for the design of an effective traffic monitoring system is to provide a high spatial density measurements. A viable solution for achieving that purpose consists of a system based on a Wireless Sensor Network (WSN) infrastructure which reduces the required investment, enables the employment in large-scale and allows future developments of systems based on multiple sensors that collaborate in collecting informations. Several wireless sensor networks have been investigated, including wireless magnetic sensors [3] [6], and acoustic vehicle detection based

on coherent cross-correlation [8].

In this paper, we propose a Wireless Sensor Network that utilizes a microphone array to detect the sound waves generated by the road vehicles. System nodes process sound signals locally to extract traffic parameters on site rather than transmitting the measurements, in order to save both in energy and in bandwidth. The basic principle of the sensing technique is to measure the temporal variation of the differential time of arrival of the acoustic signal at each pair of sensors with an algorithm based on a generalized cross-correlation method. The collected information are transmitted to a central server and made available to a remote user. In comparison with existing traffic sensors, the proposed system offers lower installation and maintenance costs, is less intrusive to environment and allows the detection of traffic congestion location.

In particular, the paper is organized as follow. An outlook of the system composition and operation is presented in Section II. Section III and Section IV describes the hardware and the basic operation of System nodes. Section V briefly present the communication protocol. Finally, in Section VI, experimental results of continuous long term operation are shown.

II. SYSTEM DESCRIPTION

Vehicle detection and traffic monitoring is an important and demanding application of WSN. The equipment and maintenance cost and time-consuming installations of existing sensing systems prevent large-scale deployment of real-time traffic monitoring and control. This leads to deployment of traffic sensors only at critical location which work independently of each other. Small wireless sensors with integrated sensing, computing, and wireless communication capabilities offer tremendous advantages in low cost and easy installation.

We propose a real-time traffic monitoring system based on a WSN infrastructure, the system allows traffic monitoring and queue detection to be performed in real-time at a larger space scale with an comparably low investment in installation and maintenance costs. The developed system is composed of two different sensor nodes having different hardware characteristics and employing different sensing techniques. The sensors work together in collecting traffic information in order to obtain an excellent spatial resolution and allow to detect the location of a traffic congestion condition (traffic jam or queue).

In Fig. 1, a basic module infrastructure deployed along the motorway is represented. This module can be spatially replicated on both side of the motorway to coverage a wide area.

The basic module of the system infrastructure is composed of a Master Node (MN), which has superior computational and energy resources and is connected to a remote database via TCP/IP over UMTS. The sound signal is detected and processed by the embedded resource of the MN using an original algorithm that allow to automatically extract *traffic parameters* on site. The information is transmitted to a central server and made available to a remote user.

The MN is wirelessly connected to a number of regularly spaced Sensor Nodes (SNs) operating on a low duty-cycle and woken-up on demand. When a queue or traffic jam is detected at the MN location the SNs are activated by the MN in order to locate the position of the queue or traffic jam, thus providing a real-time picture of the traffic flow sampled at the same space interval as the SN deployed on the motorway.

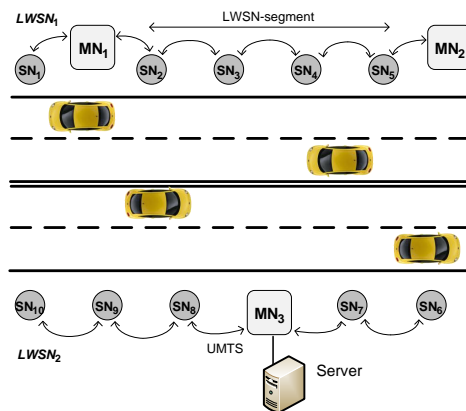


Fig. 1. Basic system infrastructure.

III. MN DESIGN AND OPERATION

Each Master Node is composed of a Sensor Unit detecting the audio signal coming from the sound sources and a Computational Unit which performs signal processing and vehicle detection while supporting at the same time the communication with both the associated SNs by the RF Unit and with the central server by the UMTS modem. The setup of the MN is packaged into a compact lightweight panel which can be easy installed at motorway's guardrail.

A. Sound Map

Figure 2 shows the arrangement of the *sensor unit*, consisting in a pair of microphones (MIC1 and MIC2), separated by $2b$ m and installed with the baseline parallel to the road. We suppose that vehicles travel on a straight path along the road, at the distance of D m, with a constant speed v_0 over the time period of interest. The time observation windows is $[-\frac{T}{2}, \frac{T}{2}]$.

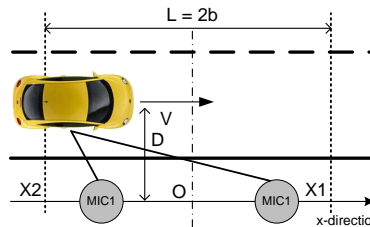


Fig. 2. MN Sensor unit setup.

Sound signals generated by traveling vehicles reach the two microphones at slightly different times due to the difference in the air path; the propagation time delay is $\tau_i = d_1(t; v_0) / c$

where c is the speed of sound in air. The two received signals can be expressed as:

$$s_1(t) = s(t) \text{ and } s_2(t) = s(t - \tau)$$

The issue of estimating the vehicle's speed can be reduced to a Time Delay Estimation (TDE) problem. The objective of TDE is to determine the relative time difference of arrival (TDOA) between signals received by a different sensor. The generalized cross-correlation (GCC) method is the most popular to do so and is well explained in an paper by Knapp and Carter [7].

The cross-correlation of the two signals function yields:

$$R_{s_1 s_2}(t) = \int s_1(t) s_2(t)(t - \tau) d\tau = s_1(t) * s_2(t) \quad (1)$$

where $*$ is the convolution operation.

The cross-correlation $R_{s_1 s_2}(t)$ obtain is maximum when $t = \tau$. So the differential time, between the two signals, can be acquired by get the maximum of the cross-correlation function.

The calculation of the cross-correlation could be done in the Fourier transform domain, thus in the digital processing it could be implemented with the FFT to reduce the computational workload. The Fourier transform of the equation is:

$$F[R_{s_1 s_2}(t)] = F[s_1(t) * s_2(t)] = S_1(f) * S_2^*(f) \quad (2)$$

Therefore, the calculation of the cross-correlation will be transformed to a Fourier transform, a multiplication and a Reverse Fourier transform of the two signals $s_1(t)$ $s_2(t)$.

In the cross-correlation domain, the position of the peak represents the time delay, and changes with the position of the source. Measuring the temporal variation of the time delay, corresponding with the position of the cross-correlation peak, in a certain observation time interval; we can create a digital Sound Map, representing the source motion along a predefined track.

A typical sound map is shown in Fig. 3; the x-axis represents the observation time and the y-axis represents the time delay τ .

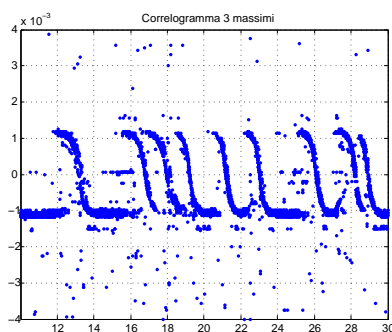


Fig. 3. Sound Map.

A vehicle passing in front of the sensor unit leaves a recognizable trace that could be described by an analytic solution, according to [8]. The shape of the curve could be

derived from the sound path difference in the air and expressed by:

$$\tau(t) = \frac{1}{c} \left[\sqrt{(x+b)^2 + y^2 + z^2} - \sqrt{(x-b)^2 + y^2 + z^2} \right] \quad (3)$$

where, c is the speed of the sound in air, d is the microphones spacing, $x = v_0 t$ is the vehicle position in the x-direction, $y = D$ is the distance between mics and vehicle, z is the height of the mics above the ground.

The problem for acoustic sensor vehicle detection is to achieve robust vehicle detection under various acoustic noise corruption, as can be observed in the sound map. Since the sensor nodes are powered by battery the solution has to be a low power demanding the development of an efficient algorithm. To achieve that goal, a solution based on a filtering band-pass and a phase correlation method has been adopted. The band pass filter is designed to remove the unwanted background acoustic and the noise, whose spectral contributions were found in the frequency domain below 500HZ.

The *phase correlation* is a GCC method, in which the transform coefficients are normalized to unit magnitude prior to computing correlation in the frequency domain. Thus, the correlation is based only on phase information and is insensitive to changes in sound intensity. Although experience has shown this approach to be successful, it has the drawback that all transform components are weighted equally, whereas one might expect that insignificant components should be given less weight.

A Sound Map after the described processing is shown in Fig. 4; if it is compared with the one of Fig. 3, a relevant improvement in the term of sharpness could be observed. An automatic traffic parameters extraction procedure, from this map, can now be developed.

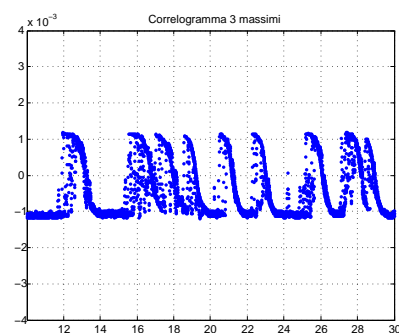


Fig. 4. Sound Map after the post-processing.

B. Parameters Extraction Procedure

In Fig. 5, a Sound Map corresponding to a single vehicle transit is reported. Multiple sound source could be processed and hence could appear in the sound map. As in a vehicle the main acoustic source is represented by vehicle tyres, each sound map for a single vehicle, would consist of two or more traces, each corresponding to a vehicle axle.

With the reference of Fig. 2, it could be observed that when the vehicle crosses the center of the setup, corresponding

to the point "O" or CPA (Closest Point of arrival) the time difference for the two signals is zero. This correspond with the crossing of the x-axis in the sound map, in the neighborhood of this point the curve can be approximated, with a straight line, and hence could be demonstrated that the trace slope is proportional to the vehicle speed.

To detect a *vehicle transit*, two symmetrical points corresponding to the positive time delay τ_1 and the negative time delay $\tau_2 = -\tau_1$ are positioned on the y-axis of the sound map (see Fig. 5). Those time delays correspond to two symmetrical positions, X1 and X2, of the vehicle along the traveling path, whose spacing is L (see Fig. 2 for reference).

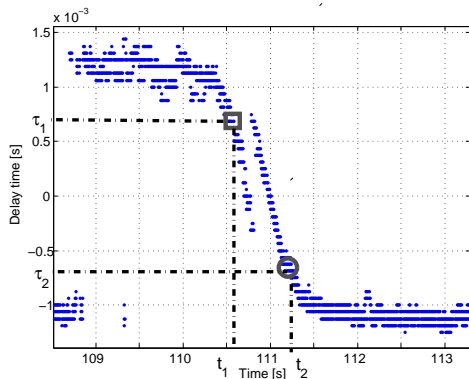


Fig. 5. Vehicle detection procedure.

A vehicle transit is detected if the sound trace intercepts in sequence the values τ_1 and τ_2 that occurs when a vehicle passes through the two virtual position X1 and X2. Therefore, as τ_1 and τ_2 are selected in the linear portion of the trace, the vehicle traveling speed, V_v , can be easy calculated, according to the following expression:

$$V_v = \frac{Lk}{t_2 - t_1} \quad (4)$$

where k is a scale factor and was estimated on a statistical basis.

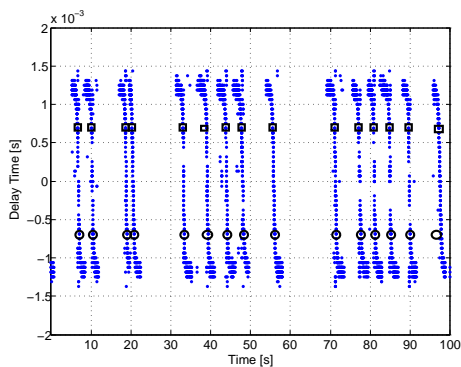


Fig. 6. Multiple detection transit.

In Fig. 6, a sound map is reported, showing the sequence of square and circle markers associated to multiple vehicle

detection obtained from the automatic procedure previously described. As it can be observed, all the passing vehicles are successfully detected in this case.

The output extraction routines are represented by some parameters indicating the traffic condition at the MN location. These parameters are related in a summary report and sent to a central server.

The previously described method for traffic parameter extraction was extensively tested during a long period of continuous operation. In Section VI, we will present results of the long term system operation.

IV. SN DESIGN AND OPERATION

According to the proposed architecture, the sensor network also includes Sensor Nodes. As previously mentioned, the main job of the SNs is to produce traffic reports on-demand for dynamically locating the position of a queue or traffic jam.

When a traffic queue or jam is detected at the MN location, the SNs associated with the MN are switched to *operative mode*, the detection of traffic conditions (fluid flow or queue) is performed through an analysis of the energy distribution features. As long as the SNs stay in the operative mode, they regularly produce a traffic report containing traffic conditions information that is passed to the MN according to a scheduling time interval. Communication between the devices is performed by a cross-layer MAC Routing protocol as described in Section V.

The MN reports the information to the central server about the traffic conditions at each individual SN; as a consequence, the *traffic flow distribution* is sampled at the same spacing interval as the SNs deployed on the motorway, thus a complete real-time picture of traffic flow is provided to the user/customer.

The detection of traffic conditions (fluid flow or queue) is performed via analysis of the energy distribution features. With reference of Fig. 7, the energy distribution of the acoustic signal associated with the traffic flow could be observed. Moving vehicles yield well defined energy peaks in the time domain, instead, standing vehicles, feature a smoother energy distribution and exhibit a much lower associated average energy.

Thus a qualitative information of a *fluid traffic* condition, is associated to the presence of isolated energy peaks, while a *queue* or *jam* condition is associated to an energy floor, with a much lower associated average energy.

The processing unit computes the energy distribution in the time domain and an algorithm based on a state machine detects the passing vehicle. According to [3], an adaptive threshold estimated on the energy value's moving average is on the basis of the *state machine*. A block diagram of the processing is shown in Figure 8.

The acoustic signal sensed by the microphone is first high-pass filtered to remove the contribution of background noise and opposite roadway vehicles noise. Due to this signal conditioning the energy revealed by the sensor is mainly associated to the vehicles traveling in the close carriageway.

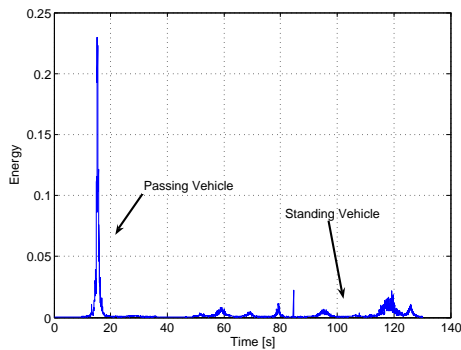


Fig. 7. Energy distribution.

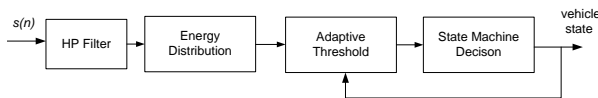


Fig. 8. Block diagram of SN operation.

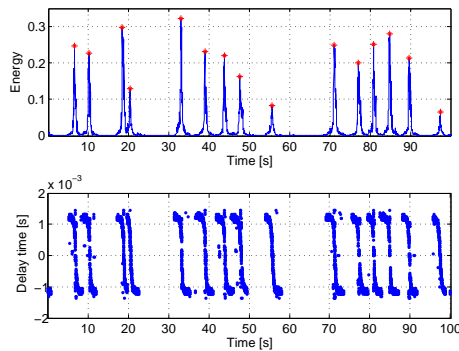


Fig. 9. Correlation between energy distribution and sound map.

Fig. 9 shows the result of this process compared with the sound map generated by the MN. It can be seen that the implemented algorithm is capable to detect, in this case, all the peaks of the energy distribution, as the vehicles are fairly spaced apart. In heavier traffic condition, however, the vehicle counting could be underestimated, but, in any case, the energy distribution represents an useful indicator to estimate the traffic flow in the carriageway.

V. PROTOCOL DESIGN

Main issues in Medium Access Control (MAC) and Routing protocol design are power consumption and the possibility of establishing a quick set-up and end-to-end communication. Other important features are scalability and adaptability of network topology, in terms of number of nodes and their density.

Taking these requirements into account, a MAC protocol and a multi-hop routing protocol were implemented. A multi-hop approach was preferred as opposed to a star topology because it also helps to realize an end-to-end communication in the presence of obstacles (i.e., flyovers, trees, curves) that

TABLE I
ROUTING TABLE GENERAL STRUCTURE

Master Node	Next Hop	Hop Count	Loop Flag
MN_1	SN_1	η_A	false
MN_1	SN_2	η_B	true
MN_2	SN_3	η_C	true

would otherwise prevent the establishment of a direct link between the SNs and the MNs.

According to the proposed MAC protocol, each node might be either in an idle mode, in which it remains for a time interval T_l (listening time), or in an energy saving sleeping state for a T_s (sleeping time). The transitions between states are synchronous with a period frame equal to $T_f = T_l + T_s$ partitioned in two sub-intervals, as shown in Fig. 10

To provide the network with full communication capabilities, all the nodes need to be weakly synchronized, meaning that they are aware at least of the awaking time of all their neighbors. To this end, a node sends an HELLO message frame by frame to each of its neighbor nodes known to be in the listening mode (Synchronous Transmission), whereas, during the setup phase in which each node discovers the network topology, the control messages are asynchronously broad-casted.

On the other hand, its neighbors periodically awake and enter the listening state independently (Asynchronous Reception). The header of the synchronization message contains the following fields: a unique node identifier, the message sequence number and the phase, or the time interval after which the sender claims to be in the listening status waiting for both synchronization and data messages from its neighbors.

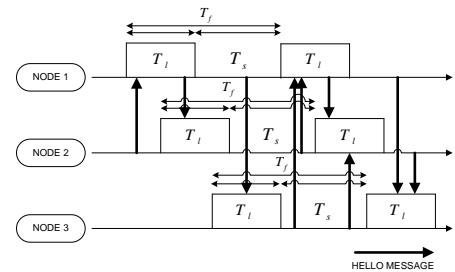


Fig. 10. MAC protocol HELLO message exchange

In order to evaluate the capability of the proposed MAC scheme in establishing effective end-to-end communications within each LWSN, a routing protocol was introduced and integrated according to the cross layer design principle [10]. It is based on sending periodical information needed for building and maintaining the local routing tables depicted in Table I.

It resorts to the signaling introduced by the MAC layer with the aim of minimize the overhead and make the system more adaptive in a cross layer fashion.

VI. EXPERIMENTAL RESULTS

First of all simulation experiments in laboratories has been performed to develop the proposed sensing method. Experi-

ments were conducted using an acoustic signal recorded at an test site with the definitive sensor unit. Results of the simulation test and analysis are shown in the previous figures.

At the same time, the design of the hardware components is been carried out, in order to select the best arrangement of a prototype basic unit, allowing the sensing and processing operations, with the best cost-performance.

Finally, the prototype basic unit, has been deployed, along the Italian highway operated by Autostrade per l'Italia SpA (ASPI) near Florence. The basic unit was first installed on May 2009; since then it is operating collecting traffic parameters and is transmitting them to a central server. The prototype unit has been placed closely to a loop detector to test the MN operation.

During the long-term operation period, the system has detected various typologies of traffic condition under many environmental and weather conditions. Also the communication modality was tested successfully.

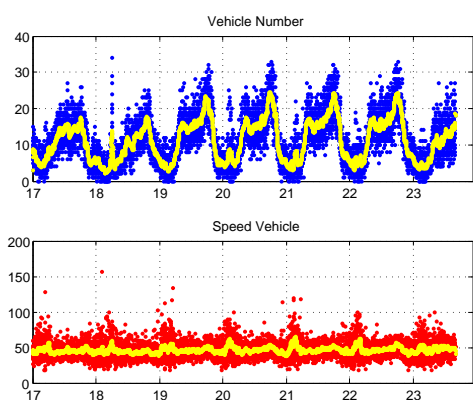


Fig. 11. Vehicle transit and average speed for a weekly observation slot.

Below, some of the collected data are presented; in Fig. 11 a weekly data collection related to vehicles transit and average speed is shown, highlighting the periodicity of the traffic flow with different behavior depending by day and hours.

The MN operation is validated by comparison with the loop detector. As is shown in Fig. 12, the two systems exhibit a good matching. The overestimation of the number of vehicles during the night is due to the background noise. For this purpose a specific post processing algorithm is under development.

The MN reports are now fully integrated in the ASPI information system. SN reports are not yet available in graphic format. Extensive tests during the period of operation have provided the motorway practitioners with a complete reporting about traffic trends. Due to the yield and easy deployment of the system, a 50 km, dual carriageway complete installation is planned by ASPI to fully exploit the potential of the system in the A1 motorway, between Florence and Arezzo.

VII. CONCLUSION

In this paper a real-time traffic monitoring system, based on acoustic WSN has been proposed. The sensing technique

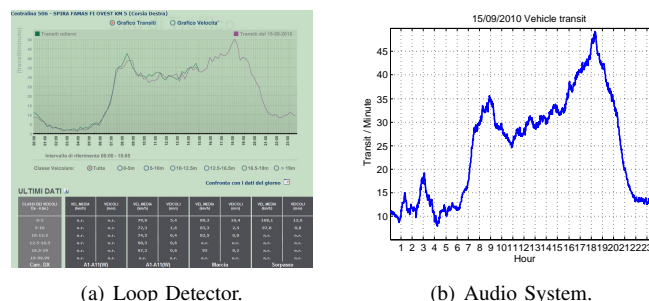


Fig. 12. Comparison between audio sensor and loop detector results.

is based on an array of acoustic sensors. The system is able to extract traffic parameters from the sound signals generated by the passing vehicles. System's nodes process sound signals locally on-site and transmit the collected information to a central server in order to be available for a remote user.

The signal processing algorithm and the vehicle detection procedure are described. Experimental results of long-time period operation are shown.

The developed system shows the following key features: (i) provides a complete picture state of the traffic flow at an larger scale and in real-time (ii) collect information coming from two different devices (iii) presents low installation and maintenance cost (iv) is able to large scale deployment.

REFERENCES

- [1] Klausner, A., Erb, S., Tengg, A., Rinner, B.: DSP Based Acoustic Vehicle Classification for Multi-Sensor Real-Time Traffic. Graz University of Technology, Graz, Austria.
- [2] Foren, J. F., Jaarsma, D.: Traffic Monitoring by Tire Noise. Proc. IEEE Conf. on Intelligent Transportation System, Boston, MA, Nov 1997, pp. 177-182.
- [3] Ding, J., Cheung, S.Y., Tan, C.-W., Varaiya, P.: Signal processing of sensor node data for vehicle detection. Seventh Int. IEEE Conf. Intell. Transp. Syst.
- [4] Lopez-Valcarce, R., Mosquera, C., Perez-Gonzalez, R.: "Estimation of road vehicle speed using two omnidirectional microphones: A maximum likelihood approach", EURASIP J. Appl. Signal Process., p.1059, 2004.
- [5] Lo, K. W., Ferguson, B. G. : "Broadband passive acoustic technique for target motion parameter estimation", IEEE Trans. Aerosp. Elect. Syst., vol. 36, p.163, 2000.
- [6] Cheung, S., Coleri, S., Varaiya, P.: Traffic Surveillance with Wireless Magnetic Sensors. University of California, Berkeley, USA
- [7] Knapp, C.H., Karter, G.C.: The Generalized Correlation Method for Estimation of Time Delay. IEEE Transactions on Acoustic Speech and Signal Processing, Vol. ASSP-24, No. 4, August 1976, pp. 320-327.
- [8] Chen, S., Sun, Z.P., Bridge, B.: Traffic Monitoring Using Digital Sound Field Mapping. IEEE Transactions on Vehicular Technology, Vol. 50, No. 6, November 2001, pp. 1582-1589.
- [9] 802.15.4-2003: part 15.4: Wireless Medium Access Control (MAC) and Physical Layer (PHY) Specifications for Low-Rate Wireless Personal Area Networks (LR-WPANs). IEEE Std., October 2003. [Online]. Available: www.ieee.org.
- [10] Shakkottai, S., Rappaport, T., Karlsson, P.: Cross-Layer Design for Wireless Networks. IEEE Comm. Mag., vol. 41, pp. 74-80, October 2003.

A Prototypical In-Car Entertainment Setup Using Software Defined Radio and Ethernet/IP-Based In-Vehicle Communication

Lothar Stolz, Kay Weckemann, and Hyung-Taek Lim

*BMW Group
Research and Technology
Munich, Germany*

{Lothar.Stolz,Kay.Weckemann,Hyung-Taek.Lim}@bmw.de

Walter Stechele

*Institute for Integrated Systems
Technical University of Munich
Munich, Germany*

walter.stechele@tum.de

Abstract—We introduce a novel approach to in-vehicle radio entertainment platforms. Using a prototypical automotive setup for car-radio reception, we evaluate a Digital Audio Broadcasting receiver implemented as a Software-Defined Radio. The radio runs as an application on a low-cost x86 device. Furthermore, we distribute the digital audio stream and control information via a standard Internet Protocol/Ethernet link instead of a proprietary automotive field bus technology. Thus, the car demonstrator distinguishes from today's approaches to automotive radio entertainment by increased flexibility on the computation as well as on the communication side, together with potential savings on costs.

Keywords-DAB, SDR, IP, Ethernet, in-vehicle networking.

I. INTRODUCTION

Radio entertainment receivers were introduced into cars as a mass product in the 1960s. For broadcasting, the scenario of FM and AM analog radio reception kept almost stable for almost 50 years. However, with the advent and progress of digital communication, the number of worldwide broadcasting standards increases steadily. New standards arise quickly and Application Specific ICs (ASICs) for radio hardware undergo revisions in short intervals of a few months. On the other hand – especially compared to consumer electronic devices – the product life cycle of automotive Electronic Control Units (ECUs) is much longer. Software-Defined Radio (SDR) describes the paradigm of implementing most of the signal processing of a radio device on a reprogrammable compute platform [1]. Hereby, a high degree of flexibility is promised as the device can adopt its signal processing to potentially any introduced transmission scheme as long as its compute resources are sufficient.

We will achieve the highest grade of flexibility, when we co-use the automotive entertainment unit's application processor instead of having a dedicated decoder IC within the platform. So, we investigate the feasibility of implementing the whole signal processing on the head unit, exemplified by a low-cost general-purpose CPU. We demonstrate an all software-defined radio receiver for digital radio broadcast being compliant to the Digital Audio Broadcasting (DAB) standard.

The in-vehicle network is currently changing due to the increasing bandwidth demand of Advanced Driver Assistance Systems (ADAS) [2]. There is a paradigm shift from the proprietary automotive bus systems to standard technology such as Ethernet to realize a communication very cost-effective. The introducing of two-wire unshielded cables with adaptive physical layer of 100 Mbit/s Ethernet makes Ethernet more interesting for the in-vehicle communication, which is considered by the OPEN ALLIANCE [3].

In this research work, we communicate over an Ethernet link instead of a proprietary automotive field bus technology. For distributing multimedia content in the automotive domain, the proprietary Media Oriented Systems Transport (MOST) field bus is employed today. We demonstrate a distributed in-vehicle audio system relying on Internet Protocol (IP)/Ethernet-based communication – a proven consumer electronics technology recently coming into focus for demanding automotive use cases [4]. For real-time audio streaming, the Real-Time Protocol (RTP) is used. The control flow is done using an IP-based Remote Procedure Call (RPC) framework. Therefore we adapted the open source solution Apache Etch [5] [6].

The remainder is structured as follows: we first introduce the three main concepts used for the components of the demonstrator and establish the relation to the presented use case from automotive domain. Afterwards, we report on the prototypical implementation of the overall system.

II. SOFTWARE DEFINED RADIO

SDR-like functionality for the mass markets are implemented mostly on dedicated Digital Signal Processors (DSPs). Shifting the signal processing to the central application processor will require a more powerful CPU. This is due to additional workload as well as to the fact that the CPU now is a general-purpose processor rather than an application specific one. However, integrating two processor systems into one will potentially save costs, and also save space on the printed circuit board.

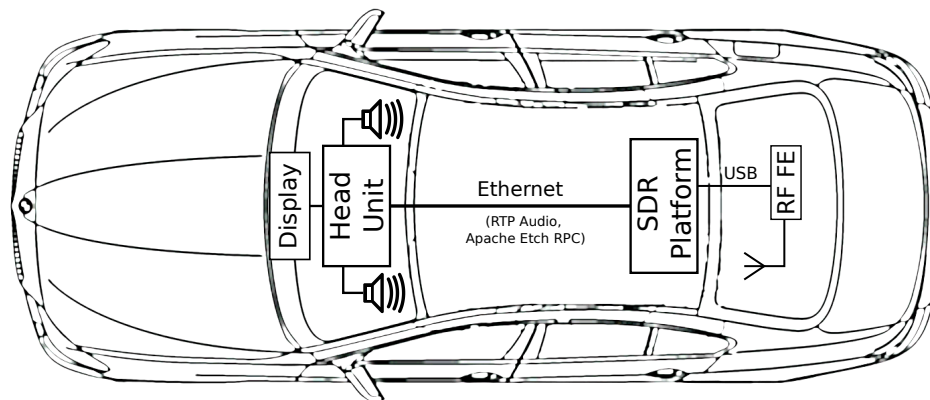


Figure 1. The test vehicle system architecture.

A. Digital Audio Broadcasting

The DAB system was introduced by the Eureka 147 working group in order to replace the analogue FM radio transmissions. It is standardized in ETIS EN 300 401 [7]. DAB is a typical representative of an OFDM-based transmission scheme. The DAB RF channel has an RF bandwidth of 1536 kHz. One channel carries an ensemble being comprised of multiple audio and/or data services. Hereby, audio data is grouped into payload chunks of 24 ms each and subsequently compressed using an MPEG 1 Layer II coder. Lately, the standard was extended to support also MPEG HE AAC as a second codec, providing state-of-the-art source encoding at reduced bit rates. This is known as the DAB⁺ system [8]. Having lots of techniques in common, DAB can be seen as an audio/high-mobility companion to the digital television system Digital Video Broadcasting Terrestrial (DVB-T),

B. The Software Demodulator

For the development of a DAB-compliant OFDM baseband signal processing chain, we follow the standard [7] and the algorithmic concepts outlined in [9] [10], and bring them to a software defined radio implementation. By extensive optimization, especially by applying hand-tuned assembler code using x86 signal processing SSE instruction set extensions, we obtain a highly optimized software radio processing chain [11]. As input, the digitized raw complex baseband is expected at a sampling rate of 2048 kSa/s. Having complex-valued samples at 16 bit each, this results in a data rate of 64 Mbit/s, which has to be provided by the RF frontend. We chose the USB interface to bridge this system component to the compute platform. Furthermore, the bus allows a distant placement of the frontend, for instance, close to the antenna, in order to minimize RF cabling losses. Table I gives the CPU load shares for the SDR part deployed to the test platform being introduced later.

Software receiver component	CPU Load*)
DAB signal processing	7.4%
RF baseband acquisition via USB	2.9%
Operating system / threading overhead	1.5%
Total	11.8%

*) at DAB service bit rate $r = 192$ kbit/s

Table I
CPU LOAD DISTRIBUTION FOR THE DAB SOFTWARE RECEIVER ON THE SELECTED LOW-COST TEST PLATFORM.

III. IP-BASED AUDIO STREAMING

Each 24 ms, one complete MPEG frame of encoded audio gets available from the DAB receiver core. The resulting payload size p in byte can be calculated by equation

$$p = \frac{1}{8} \cdot 24 \text{ ms} \cdot r \quad (1)$$

where r is the bit rate of the received DAB audio service stream. Assuming an exemplary bit rate of 192 kbit/s for instance, we will encounter a consistent MPEG frame size of 576 byte.

The Real-Time Protocol is being defined in RFC3550 [12]. Basically, it adds time stamp data to allow the information sink to provide on-time presentation

Protocol	Header Size
Ethernet*)	18 byte
IP	20 byte
UDP	8 byte
RTP	12 byte
Total	58 byte

*) no VLAN-tag.

Table II
ABSOLUTE DATA OVERHEAD INTRODUCED BY RTP/IP-BASED AUDIO STREAMING OVER ETHERNET.

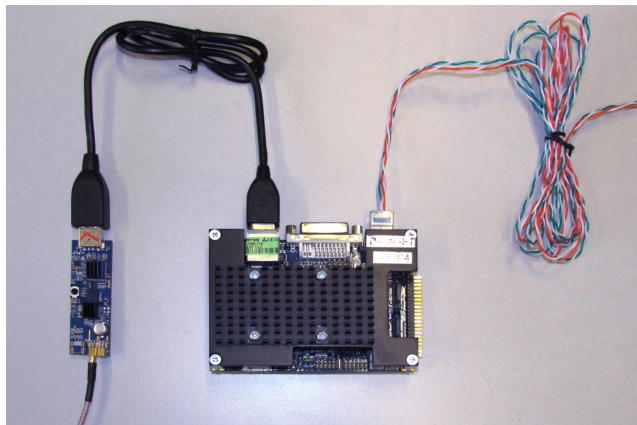


Figure 2. The SDR platform connects via USB to the RF-preamplifier/frontend, and via Ethernet over unshielded twisted pair to the head unit emulator.

Audio Rate r	Overhead
64 kbit/s	30.2%
96 kbit/s	20.1%
128 kbit/s	15.1%
192 kbit/s	10.1%
256 kbit/s	7.6%

Table III

RELATIVE DATA OVERHEAD INTRODUCED BY RTP/IP-BASED AUDIO STREAMING OVER ETHERNET FOR TYPICAL DAB AUDIO BIT RATES r .

of content and to cope with loss of data. Due to the IP protocol stack hierarchy, overhead is introduced by the packet headers of all corresponding layers: Ethernet, IP, UDP and RTP headers together add 58 byte to each packet (see Table II), which increases the effective total streaming rate r_{total} on Ethernet frame layer by 19.33 kbit/s.

$$r_{\text{total}} = r + \frac{58 \cdot 8 \text{ bit}}{24 \text{ ms}} = r + 19.33 \text{ kbit/s} \quad (2)$$

Again assumed for an exemplary audio rate of 192 kbit/s, the IP-based audio transport approximately adds 10% of bandwidth due to protocol overhead (Table III).

Such overhead could potentially be decreased by grouping packets of multiple 24 ms MPEG frames, however adding latency in exchange. For an audio service rate $r = 256$ kbit/s being presumed as the maximum rate, r_{total} is 275 kbit/s. This is well feasible on an 100 Mbit/s Ethernet link.

Ethernet frames are limited in size by the so-called Maximum Transmission Unit (MTU). The payload must have no more than 1500 byte, otherwise it must be fragmented on higher protocol layers. For $r = 256$ kbit/s, a complete 24 ms audio packet will have a size of $p = 768$ byte plus the headers of IP, UDP, RTP (40 byte). This is well below the MTU value, thus no fragmentation is needed.

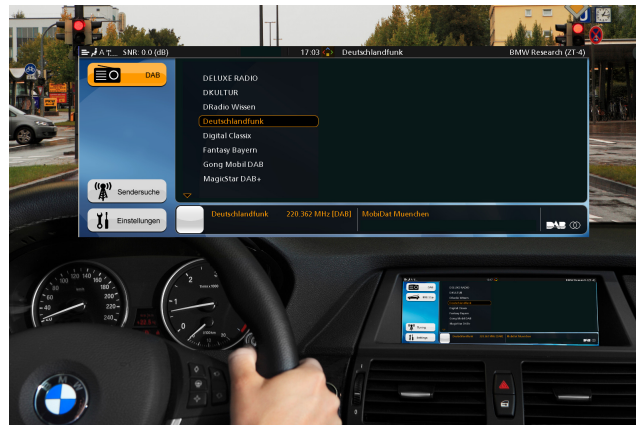


Figure 3. The head unit emulator uses an embedded PC similar to the SDR platform. The graphical user interface is integrated to the car HMI.

IV. IP-BASED MIDDLEWARE

Besides the streaming data, the prototypical receiver implementation has to announce station lists to and receive tuning commands from a distant controller – in general the Human Machine Interface (HMI). Middleware abstracts the communication from the application. Following a definition from Issarny et al. [13], middleware defines an Interface Description Language (IDL), a high-level addressing scheme, a coordination model based on an interaction paradigm and semantics, a transport protocol, and a naming and discovery protocol including conventions to publish and discover resources. The concept of Remote Procedure Calls as interaction paradigm fulfills the required functionality well. For the prototype, we used the open source RPC framework Apache Etch [5]. As the existing Apache Etch bindings primarily target fully-featured workstations, we implemented our own light-weight binding that is targeted at embedded computing requirements [14].

V. CAR RADIO RECEIVER PROTOTYPE AND PRELIMINARY RESULTS

As we focus on low-cost platforms, the compute platform selected for the prototype is based on the Intel Atom single core CPU (Table IV). As working memory, 512 MB of RAM are mounted. A prototypical RF frontend peripheral is located close to the antenna and connected point-to-point via USB bus to the SDR platform. The antenna input signal is mixed down to baseband, digitized and sent to the SDR host.

To demonstrate the distribution between a head unit ECU as sink and an external tuner ECU as source, we use Ethernet over a pair of unshielded twisted pair cables (U/UTP). Within this setup, the associated head unit is emulated by an identical x86 platform. Via an LVDS-converter the in-car display is connected. Furthermore, the car's main haptic controller *iDrive* is attached by a Controller Area Network

Platform	Intel Atom
CPU micro architecture	x86 in-order (“Bonnell”)
No. of cores	1
Core clock	1600MHz
DRAM type	DDR2-667, single ch.

Table IV
TEST PLATFORM USED FOR PROFILING.

System Component	Occupied Resources
CPU Load	
DAB SDR Receiver (Tuner)	up to 15%*
MPEG Audio Playback (Head Unit)	up to 6%*
Bus Load	
Audio Streaming Bus (Ethernet)	up to 275 kbit/s*
RF Frontend Bus (USB)	64 Mbit/s

*) depending on actual DAB service bit rate $r \leq 256$ kbit/s

Table V
DEMAND OF RESOURCES FOR THE PRESENTED DEMONSTRATOR SETUP.

(CAN) adapter. To receive, decode and playback the MPEG audio stream, the head unit setup relies on the Videolan VLC framework. Analog audio output is brought by auxiliary line input to the in-car sound amplifier.

Table V summarizes the required system resources for the prototypical setup of this use case.

VI. CONCLUSION AND FUTURE WORK

We presented a test vehicle-integrated prototype of a real-time DAB receiver as a novel approach to automotive in-vehicle entertainment: rather than using custom protocols from the automotive domain and proprietary application specific ICs, software solutions and open standards from consumer electronics were evaluated. We proved that real-time/on-air radio signal processing using software-based demodulation turns out to be possible at reasonable load on a general-purpose CPU for a digital broadcasting receiver. Furthermore, we showed that stable in-vehicle distribution of audio and control relying on IP and Ethernet is feasible. The results gained in the entertainment/broadcast audio domain encourage the evaluation of other use cases. Ongoing activities in the field of future IP-based in-vehicle network architecture will be continued. Studies on SDR evaluation will be intensified and extended from unidirectional broadcast radio to bidirectional data communications to derive further in-depth knowledge.

REFERENCES

- [1] W. Tuttlebee, *Software-defined radio: facets of a developing technology*, IEEE Personal Communications, Vol. 6, pp. 38–44, 1999.
- [2] H.-T. Lim, B. Krebs, L. Völker, and P. Zahrer, *Performance Evaluation of the Inter-Domain Communication in a Switched Ethernet Based In-Car Network*, 36th Annual IEEE Conference on Local Computer Networks (LCN), pp. 101–108, Bonn, Oct. 2011.
- [3] OPEN Alliance, *OPEN Alliance SIG*, [Online]. Available: <http://www.opensig.org/about.php> [Mar. 2012].
- [4] L.L. Bello, *The Case for Ethernet in Automotive Communications*, Special Issue on the 10th International Workshop on Real-Time Networks, Vol. 8. No. 4, 2011.
- [5] Apache Etch community, *Apache Etch*, [Online]. Available: <http://incubator.apache.org/etch> [Feb. 2012].
- [6] K. Weckemann, H.-T Lim, and D. Herrscher, *Practical experiences on a communication middleware for IP-based in-car networks*, Proceedings of the International Conference on Communication System Software and Middleware (COM-SWARE), Verona, Italy, 2011.
- [7] ETSI, *Radio Broadcasting Systems: Digital Audio Broadcasting to mobile portable and fixed receivers* ETSI EN 300 401 V1.4.1, European Telecommunications Standards Institute, Jan. 2006.
- [8] ETSI, *Digital Audio Broadcasting (DAB); Transport of Advanced Audio Coding (AAC) Audio*, ETSI TS 102 563 V1.2.1, European Telecommunications Standards Institute, May 2010.
- [9] F. van der Laar, N. Philips, and J. Huisken, *Towards the next generation of DAB receivers*, EBU Technical Review Summer 1997, pp. 46–59.
- [10] K. Taura, M. Tsujishita, M. Takeda, H. Kato, M. Ishida, and Y. Ishida, *A digital audio broadcasting (DAB) receiver*, IEEE Transactions on Consumer Electronics, Vol. 42, No. 3, pp. 322–327, Aug. 2002.
- [11] L. Stolz, M. Feilen, and W. Stechele, *An Optimized Software Defined DAB Receiver for x86 Platforms*, Proceedings of the Workshop on Software Radio, Vol. 8, Karlsruhe, Mar. 2012.
- [12] H. Schulzrinne, S. Casner, R. Frederick, and V. Jacobson, *RTP: A Transport Protocol for Real-Time Applications*, RFC 3550, Internet Engineering Task Force, July 2003.
- [13] V. Issarny, M. Caporuscio, and N. Georgantas, *A Perspective on the Future of Middleware-based Software Engineering*, Proceedings of the Future of Software Engineering, 2007.
- [14] K. Weckemann, F. Satzger, L. Stolz, D. Herrscher, and C. Linnhoff-Popien, *Lessons from a Minimal Middleware for IP-Based In-Car Communication*, to appear in: Proceedings of the IEEE Intelligent Vehicles Symposium, 2012.

Model, analysis, and improvements for V2V communication based on 802.11p

Tseesuren Batsuuri
SI Department
MCS electronics, MCS group
Ulaanbaatar, Mongolia
tseesuren.b@mcs.mn

Reinder J. Bril
Mathematics and Computer Science
Eindhoven University of Technology
Eindhoven, The Netherlands
r.j.bril@tue.nl

Johan J. Lukkien
Mathematics and Computer Science
Eindhoven University of Technology
Eindhoven, The Netherlands
j.j.lukkien@tue.nl

Abstract—Future vehicle active safety applications will rely on one-hop Periodic Broadcast Communication (oPBC) based on a new standard IEEE 802.11p. In this work, we first aim at understanding the behavior of such oPBC under varying load conditions by considering three important quality aspects of vehicle safety applications: reliability, fairness, and delay. Second, we investigate possible improvements of these quality aspects. Our evaluation reveals that the Hidden Node (HN) problem is the main cause of various quality degradations especially when the network is unsaturated. We propose three simple but effective broadcasting schemes to alleviate the impact of the HNs.

Keywords—One-hop periodic broadcast; vehicle-to-vehicle communication, 802.11p

I. INTRODUCTION

Vehicle safety applications will use two basic communications: event-driven and time-driven. In the former case, a vehicle starts broadcasting a message for a certain duration periodically when a hazardous situation is detected and, hence, the messages are not sent in normal situation. In the latter case, each vehicle continuously performs oPBC to pro-actively deliver a beacon message to the neighboring vehicles to make each vehicle aware of its vicinity such that safety applications will leverage this to detect any hazardous situation in a timely manner. A lane change advisor and collision warning applications [1] are two typical examples which require a frequency of 10 messages per second with a maximum no message interval of [0.3sec,1.0sec] [1], [2], [3]. In addition, the applications pose a strict fairness requirement [4], [5], where each vehicle should have equal opportunity. In this type of system, message loss is unavoidable (we explain the causes below); however, it must not be the case that one or a few vehicles take all the loss, because this would result in these vehicles becoming invisible to their surrounding vehicles.

When stations broadcast rather than making peer-to-peer communication the 802.11p's DCF does not use its full functions [6]. As a result, when all stations use broadcast-based communication, the collision problems, i.e., the contention and the HN problems increase. The purpose of our research is to understand the behavior of this oPBC based under varying load conditions by considering three quality

aspects which are important for vehicle safety applications: *reliability* (i.e., successful message reception ratio), *fairness* (i.e., distribution of successful message reception ratio over vehicles) and *delay* (i.e., no message interval between two vehicles that are in their CRs.). In addition, we want to investigate possible improvements. The remainder of the paper is organized as follows. Section II introduces the mathematical model. Section III presents our evaluations. Section IV presents our improvements and Section V gives a conclusion.

II. MODEL OF OPBC

Here, we encounter two aspects: a simulation of the movement of the vehicles and a simulation of the behavior of the wireless communication as a function of the position of the vehicles. Thus we have the *traffic model* which yields the position of vehicles as a function of time and the *communication model* that describes the communication events between vehicles as a function of time and vehicle location. Hence, the communication model uses the traffic model's output as one of its input parameters. The interface between the two models is formed by the location of the vehicles. Together with the radio channel model this yields the *neighborhood* structure viz., a set of vehicles that each vehicle can transmit to or receive from at any point in time. The traffic model can be very advanced, even to the extent that life traces are simulated [7]. In this work we are not concerned, however, with the traffic model and we stick to a simple highway model, represented as a stretch of several kilometers with three lanes per direction and periodic boundary conditions (which makes it, in fact, a loop). Speeds per lane are assumed to be fixed. In simulations the main concern of the traffic model is to simulate with a small enough time step to have a realistic and sufficiently accurate description for the communication model. The motivation for this restriction is that we want to study just the communication model under varying load conditions. The communication model has two parts: First, communication and radio channel model that generates the events. Second, timing model of communicating vehicles to define the concepts of interest.

1) *The communication and the radio channel model:*

We restrict ourself to describing the broadcast mode of the 802.11p DCF. Besides, we take a Signal to Interference plus Noise Ratio (SINR) based signal reception model of the updated NS-2 implementation of the 802.11p [8]. In addition, we choose the Two-Ray Ground (TRG) signal propagation model in order to study solely the effect of message collisions.

2) *The timing model:* We assume a set V of N vehicles v_1, v_2, \dots, v_N periodically broadcasting messages. The behavior of the system is described as a series of events happening at certain times. As a convention we use a superscript to denote a k^{th} occurrence or instance. For example, $e^{(k)}$ denotes the k^{th} occurrence of an event e and $m_i^{(k)}$ denotes the k^{th} message of v_i . In addition, we often do not name the event but only the time of occurrence using a similar notation, as explained next. The activation time $a_i^{(k)}$ is the time at which v_i becomes ready to broadcast $m_i^{(k)}$. The start time $s_i^{(k)}$ and finish time $f_i^{(k)}$ are the times at which v_i actually starts and finishes the transmission of message $m_i^{(k)}$, respectively. Note, from a receiver vehicle's perspective, the start time and the finish time at which the vehicle starts and finishes receiving the message $m_i^{(k)}$ are $s_i^{(k)} + \delta$ and $f_i^{(k)} + \delta$, respectively. δ is an air propagation delay that is relatively small¹, therefore we neglect this in our model. The transmission interval $tI_i^{(k)}$ of message $m_i^{(k)}$ is defined as

$$tI_i^{(k)} \stackrel{\text{def}}{=} [s_i^{(k)}, f_i^{(k)}]. \quad (1)$$

We require that

$$a_i^{(k)} < s_i^{(k)} \leq f_i^{(k)} \leq a_i^{(k+1)} \quad (2)$$

holds. Message transmission is assumed to be periodic. If a message is not sent at all or is delayed such that the remaining part of the interval is not enough for successful completion we say that the message is dropped. This may mean a partial message transmission or, in the extreme case, no transmission at all ($s_i^{(k)} = f_i^{(k)}$). In both cases, we define $f_i^{(k)} = a_i^{(k+1)}$ and we take that as the condition of message dropping. Moreover, we define transmission power $Pt_i(t)$ of vehicle v_i and its reception power at vehicle v_j as $Pr_{ij}(t)$ and cumulative reception power $cPr_j(t)$ of vehicle v_j at time t . Note, we always assume that $i \neq j$ holds whenever we talk about two vehicles v_i and v_j . We require that $Pt_i(t) > 0$ holds during $tI_i^{(k)}$ and its value is determined by the application. $Pr_{ij}(t)$ is determined by a given signal propagation model, by $Pt_i(t)$ and by the distance between sender and receiver at time t . $cPr_j(t)$ is determined by all receiving signal strengths at v_j at time t plus a noise floor, nF , as follows

$$cPr_j(t) = nF + \sum_{v_i} \{Pr_{ij}(t) | Pr_{ij}(t) \geq PsTh\}, \quad (3)$$

¹ $\delta \ll 1\mu s$ [9], [10]

where $PsTh$ is a Power Sense threshold of the receiver. Given these notions, we define the neighborhood of a vehicle. At any time t , each vehicle v_i has a target neighbor set of other vehicles, $Nb_i(t)$, where $v_j \in Nb_i(t)$ means that v_j is in the CR of v_i at time t . It is defined as follows

$$v_j \in Nb_i(t) \stackrel{\text{def}}{=} \frac{Pr_{ij}(t)}{nF} \geq SrTh, \quad (4)$$

where $SrTh$ is a SINR threshold for receiving the message successfully. Note, CR is the reception range, the places where the message could be received disregarding interference of other stations. A necessary condition for receiving a message is that the receiving vehicle must be in the CR of the sending vehicle for the duration of the message transmission. A sufficient condition for a message reception is that the receiving signal power must be equal to or greater than $SrTh$ with respect to the cumulative power of all other signals for the entire duration of the message transmission. This is defined as follows

$$\forall t : t \in tI_i^{(k)} \wedge \frac{Pr_{ij}(t)}{(cPr_j(t) - Pr_{ij}(t))} \geq SrTh. \quad (5)$$

We extend the concept of a neighborhood to intervals by

$$\downarrow Nb_i(I) = \bigcap_{t \in I} Nb_i(t). \quad (6)$$

This interval represents all vehicles that have been in the CR of vehicle v_i during the entire interval I . Changes of neighbor sets are represented by enter and leave events. Entering time $e_{ji}^{(k)}$ is the time at which v_j enters the CR of v_i for the k^{th} time while leaving time $l_{ji}^{(k)}$ is the time at which v_j leaves the CR of v_i for the k^{th} time. The k^{th} encounter interval $eI_{ij}^{(k)}$ of v_j with v_i is defined as

$$eI_{ij}^{(k)} \stackrel{\text{def}}{=} [e_{ji}^{(k)}, l_{ji}^{(k)}]. \quad (7)$$

During $eI_{ij}^{(k)}$ we say that there is a link from i to j and we call that the k^{th} such link.

Message loss: The most important concern is whether messages are actually received by vehicles that could receive them. Considering message $m_i^{(k)}$ there are three reasons why another vehicle v_j might not receive it.

(*OOR*) *Out Of Range.* In order for a vehicle v_j to receive $m_i^{(k)}$ it must be in the neighborhood of v_i for the duration of the transmission. When $v_j \notin \downarrow Nb_i(tI_i^{(k)})$, v_j does not receive $m_i^{(k)}$.

(*MD*) *Message Dropping.* This happens, as described above, if the back-off interval becomes so long that the message transfer time does not fit in the remaining part of the period. In our model this is equivalent to

$$f_i^{(k)} = a_i^{(k+1)}. \quad (8)$$

No vehicle will receive message $m_i^{(k)}$.

(*MC*) *Message Collision.* The message is transmitted but

not received by v_j since other vehicles may transmit at the same time to v_j and their interferences are strong enough to corrupt the receiving message of v_i . This is defined as follows

$$\exists t : t \in tI_i^{(k)} \wedge \frac{Pr_{ij}(t)}{(cPr_j(t) - Pr_{ij}(t))} < SrTh. \quad (9)$$

Given these reasons for loss we define the *transmission condition* of message $m_i^{(k)}$ and, accordingly, the *reception condition* of $m_i^{(k)}$ by a vehicle v_j as follows

$$Tc_i^{(k)} = \begin{cases} MD & \text{if (8)} \\ XMT & \text{otherwise} \end{cases} \quad (10)$$

$$Rc_{ij}^{(k)} = \begin{cases} OOR & \text{if } v_j \notin \downarrow Nb_i(tI_i^{(k)}) \\ MC & \text{if } v_j \in \downarrow Nb_i(tI_i^{(k)}) \wedge (9) \\ Tc_i^{(k)} & \text{otherwise.} \end{cases} \quad (11)$$

If $Tc_i^{(k)} = XMT$, message $m_i^{(k)}$ is broadcast successfully. If $Rc_{ij}^{(k)} = XMT$, the message is received by vehicle v_j at time $f_i^{(k)}$ successfully.

Metrics: We define the most appropriate metrics that can judge the communication quality in the following three aspects: *reliability*, *fairness* and *delay*. For the *reliability* aspect, we use the fraction of successfully delivered messages (*SMR*, successful message ratio). This concept can be refined to links between vehicles and to individual messages. To start we define the number of received messages from v_i by v_j in a given interval, as well as the number of times that such message could have been received.

$$Rs_{ij}(I) = |\{k \mid tI_i^{(k)} \subseteq I \wedge Rc_{ij}^{(k)} = XMT\}| \quad (12)$$

$$Ns_{ij}(I) = |\{k \mid tI_i^{(k)} \subseteq I \wedge Tc_i^{(k)} = XMT \wedge v_j \in \downarrow Nb_i(tI_i^{(k)})\}| \quad (13)$$

The ratio is the successful message ratio in that interval.

$$SMR_{ij}(I) = \begin{cases} \frac{Rs_{ij}(I)}{Ns_{ij}(I)} & \text{if } Ns_{ij}(I) > 0 \\ 0 & \text{if } Ns_{ij}(I) = 0 \end{cases} \quad (14)$$

Generalizing this by summing over the receiving vehicles gives the successful message ratio of v_i in an interval.

$$SMR_i(I) = \begin{cases} \frac{\sum_{v_j} Rs_{ij}(I)}{\sum_{v_j} Ns_{ij}(I)} & \text{if } \sum_{v_j} Ns_{ij}(I) > 0 \\ 0 & \text{if } \sum_{v_j} Ns_{ij}(I) = 0 \end{cases} \quad (15)$$

As a special case, $SMR_i(tI_i^{(k)})$ is the *SMR* of $m_i^{(k)}$. Again, generalizing by summing over the sending vehicles we obtain the *SMR* of the entire network during that interval.

$$SMR(I) = \begin{cases} \frac{\sum_{v_i, v_j} Rs_{ij}(I)}{\sum_{v_i, v_j} Ns_{ij}(I)} & \text{if } \sum_{v_i, v_j} Ns_{ij}(I) > 0 \\ 0 & \text{if } \sum_{v_i, v_j} Ns_{ij}(I) = 0 \end{cases} \quad (16)$$

At the network level an interesting question is: how does $SMR([0, T])$, where T represents a time of consideration, behave as a function of vehicle density? From the *fairness* perspective, the behavior of individual vehicles is more important than the average. This is why we also analyze SMR_i to see whether losses are distributed evenly (or fairly) over the vehicles. The cumulative distribution function shows this; a fair distribution would give a transition from 0 to 1 within a short interval.

$$cdfSMR(I, x) = \frac{|\{v_j \mid SMR_j(I) \leq x\}|}{N}, \text{ for } 0 \leq x \leq 1 \quad (17)$$

In addition, plotting SMR_i as a function of time gives insight in the visibility of v_i for other vehicles. Finally, from the *delay* perspective, an important further question is how losses of a particular vehicle are distributed in time and across vehicles: do losses happen in sequences and do they affect the same links? To that end we define the concept of a “No Message Interval” between two vehicles during a given interval I which is the length of the longest subinterval of I without a successful message transmission.

$$NoM_{ij}(I) = \sup \{|J| \mid J \subseteq I \wedge Rs_{ij}(J) = 0\} \quad (18)$$

In addition, the “First Delay” is the length of the longest initial subinterval and represents a delay in discovery in case we apply it to an encounter interval.

$$FD_{ij}([a, b]) = \sup \{x \mid [a, a+x] \subseteq [a, b] \wedge Rs_{ij}([a, a+x]) = 0\} \quad (19)$$

In our analysis we look at genuine *NoM* and *FD*, viz., those that correspond to encounter intervals. These are examined as a function of their length and plotted as a density (histogram) or as a cumulative distribution.

III. EVALUATION OF OPBC UNDER CSMA/CA

For the purpose of this evaluation, two different scenarios are simulated. In the first scenario (single domain (SD)), vehicles are deployed at fixed locations within a single CR viz., all vehicles can receive each others messages. This scenario allows us to study the collisions caused only by the contention problem, i.e., NN collisions since there are no HNs. In the second scenario (multi domain (MD)), vehicles are deployed on a 3km long highway with three lanes per direction. This scenario allows us to study both HN and NN collisions. By having these two scenarios, we can compare the impact of these two types of collisions. The vehicles at the three lanes have fixed velocities of 20, 30, and 40 m/s respectively. In both scenarios, different inter-vehicle spacings are used in order to create different *Vehicle Densities* (VD). We assume a single channel, a fixed broadcasting period and initially, a random phasing within this period as

$$a_i^{(k)} \stackrel{\text{def}}{=} \phi_i + kT_i. \quad (20)$$

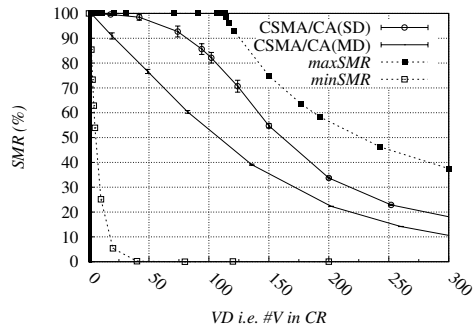


Figure 1. Successful Message Ratio (SMR) of the entire network with respect to the vehicle density (VD) shows the reliability. $maxSMR$, $minSMR$ are the max and min possible SMR, the former is calculated analytically and the latter is obtained through simulations. SD (Single Domain) case shows SMR degradation only due to the contention problem since all vehicles are deployed at fixed locations within a single CR (i.e., no HNs). MD (Multi-Domain) shows SMR degradation due to both the contention and HN problems (vehicles are deployed on a 3km long highway). $CI = 99\%$.

Thus, each v_i has a broadcasting period $T_i \in \mathbb{R}^+$ and an initial broadcasting phase $\phi_i \in \mathbb{R}^+$, where ϕ_i is uniformly selected from an interval of $[0, T_i)$. Moreover, we assume the same signal strength (300m), the same broadcasting period (0.1seconds), the same message size (555 bytes) fixed over time for all vehicles. The evaluation is based on 1 minute of simulation.

Simulation results: First, we study the reliability by means of the successful message reception ratio metric, i.e., $SMR([0,60])$. The SMR of the overall network with respect to VD of the SD and MD cases are shown in Figure 1. For each different VD case, we performed ten simulations with a different random seed for selecting the initial phases. Figure 1 presents the average values of these simulations with a confidence interval of 99%. In addition, the theoretical maximum SMR ($maxSMR$) is plotted to show the upper boundary. This $maxSMR$ is given by

$$maxSMR(VD) = \begin{cases} 1 & \text{if } VD \leq SP \\ SP/VD & \text{otherwise} \end{cases}, \quad (21)$$

where SP is the channel saturation point, i.e., the maximum capacity of the channel in terms of the number of vehicles that can fit in one period duration without any overlap in time for broadcasting. SP is given as

$$SP = \frac{T}{T_s + T_d}, \quad (22)$$

where T_s is the inter-frame space, i.e., an AIFS duration, and T_d is the time to transmit a single message. When all vehicles are optimally synchronized over the period for broadcasting, the SMR should approach this $maxSMR$ level. Besides, we obtained the minimum possible SMR level ($minSMR$) by means of simulations in which we defined roughly the same phases for all vehicles. From Figure 1, the HN problem appears to be the main cause of SMR degradation when the network is unsaturated. Once the network load exceeds its maximum capacity, the NN collisions start occurring

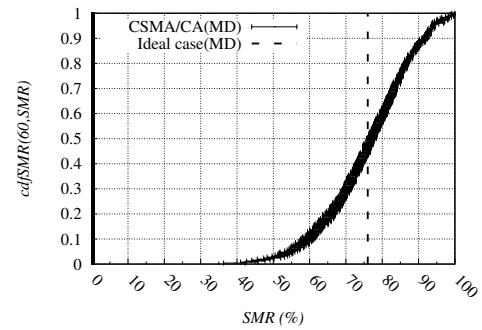


Figure 2. This shows the fairness through CDF of vehicles by their SMR. In the graph, a point indicates that $y\%$ of vehicles have at most $x\%$ SMR. In an ideal fair case, the dashed line is expected where all vehicle should have the same SMR that is equal to SMR of the entire network. $VD = 50$, $CI = 99\%$

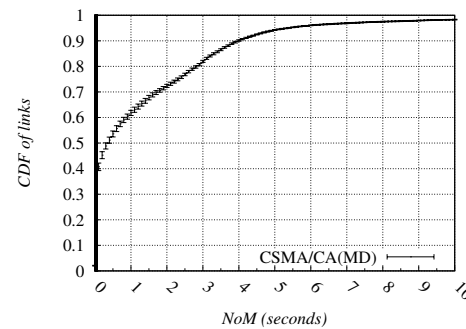


Figure 3. CDF of links by their NoM (the longest no message interval). In the graph, a point indicates that $y\%$ of links have at most x seconds of NoM. $VD = 50$, $CI = 99\%$.

in bursts thus yielding lower SMR. We now continue our study at individual vehicle level to investigate the fairness. Here, we select an unsaturated network condition where the traffic density is sparse, i.e., VD is about 50 vehicles (that corresponds to about 85 vehicles per km over 6 lanes in our settings). Figure 2 shows a relatively unfair distribution of message receptions over vehicles where some vehicles have a high SMR whereas others have a relatively low SMR. In an ideal fair case, the dashed line is expected where the distance between the best and worst cases should be close to 0, however, the fact is 65%. Figures 3 and 4 show the impact of the collision problems on the delay aspects at the link level through a cumulative distribution of links by their NoM and a histogram of links by their FD respectively. During 60 seconds of simulation ($VD=50$), approximately 53000 links are established in total. Note, the link is an one-way relationship. Some vehicles join the CR of a vehicle whereas some may leave the CR due to the relative speed between the vehicle and its neighbors. From Figure 3, we can see that almost 30% of links experience more than one second of NoM. This implies that a certain vehicle does not receive a sequence of messages from another vehicle although the vehicle could have received these messages in the absence of interferences. From Figure 4, many vehicles, i.e., about 350 ± 50 are seen that did not even discover

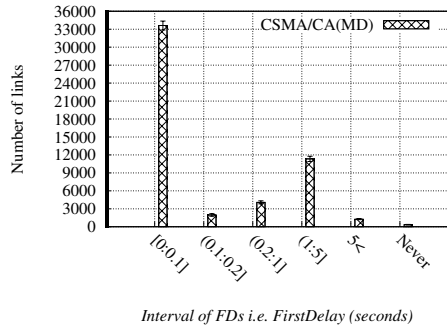


Figure 4. Distribution of links by their FD (delay to discover a new neighbor). The graph presents 5 different intervals of FD. The last interval “Never” means that some vehicles never discover its neighbors. The number of links for “5<” and “Never” are 1280 ± 95 and 350 ± 50 , respectively. $VD = 50$, $CI = 99\%$.

some of their one-hop neighboring vehicles for their entire encounter interval. Based on the above results, we conclude that HN problem is the main cause of the *SMR* degradation when the network is unsaturated. Once it is saturated, the NN problem reduces the *SMR* dramatically. Therefore, the latter one is more a network congestion problem. In fact, this congestion problem is well-known and addressed in many works, e.g., [3], [5], and [11]. The main approaches are to reduce beacon generation rate, beacon size, or to reduce the CR which are indeed all derived from (22). The impact of the HN problem is clearly revealed by an unfair *SMR* distribution and the delay characteristics such as *NoM* and *FD* mainly due to synchronized HNs, because vehicles traveling on a highway, particularly those traveling in the same direction could have a rather static topology for a relatively long period². In that topology, some vehicles could be incidentally synchronized as HNs which leads to a systematic message loss.

IV. SOLUTION FOR IMPROVING THE QUALITY OF OPBC

We look at situations where the traffic density is moderate or sparse, i.e., unsaturated. We assume that in that situation message loss is even more serious in terms of safety since the vehicles have relatively higher speeds. Therefore, such situations should have even stricter requirements on the communication.

Elastic scheme (ES): In ES, the initial phase of broadcasting is changed at a regular basis. The message activation time is defined as follows

$$a_i^{(k)} \stackrel{\text{def}}{=} \begin{cases} \phi_i & \text{if } k = 0 \\ a_i^{(k-1)} + T_i & \text{if } k > 0, \\ & (k + \phi_e) \bmod er_i \neq 0 \\ a_i^{(k-1)} + r(2T_i) & \text{if } k > 0, \\ & k \bmod er_i = 0 \end{cases} \quad (23)$$

²When CR is 300m, two vehicles approaching each other from the opposite directions with a relative speed of 80m/s will have an encounter interval of 7.5s.

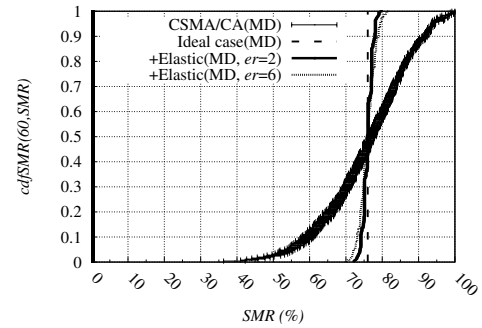


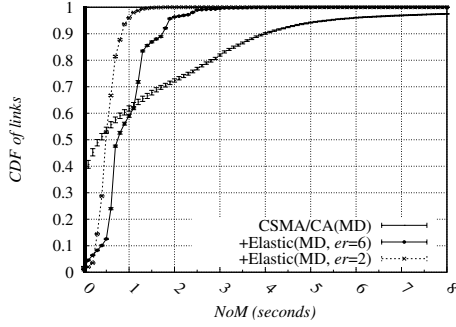
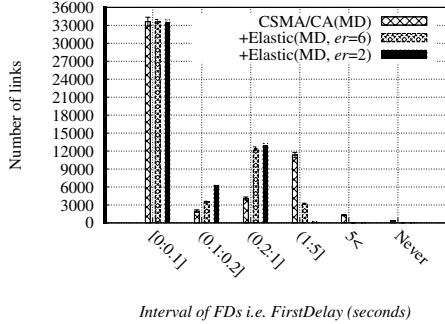
Figure 5. ES improves the fairness drastically ($VD = 50$, CI of 99%, for ES, $CI = \pm 0.3$).

where er_i is the elastic rate that defines how often the phase should be changed and r is a function that returns a random value within the given interval. This value defines how much the phase should be changed. ϕ_e is a phase for starting elasticity and it is given as $\phi_e = \lfloor r(er_i) \rfloor$. To keep the expected number of generated messages the same as the strict periodic scheme, $2T_i$ is selected as the interval. The worst case delay between two messages is $2T_i$. Figure 5, 6, and 7 show the results of this scheme in which we use the same er for all vehicles. From these graphs, we can make several interesting observations. First, it is clearly seen that the more often the phase is changed, the better the elastic scheme improves the fairness and the delay characteristics. Particularly, the fairness is improved drastically even at the higher value of er which is in result of frequent change of phasing in the elastic scheme that changes the channel condition for the vehicle. Under changing channel condition, the lifetime of a synchronized period of the vehicles (also a period of favorable channel condition of the vehicle) becomes shorter, i.e., highly likely to be at most the er period. Figure 6 reflects the effect of the short living synchronization when er is 6; we see somewhat discrete and step-like effects. As a result, each vehicle experiences more or less the same fluctuating channel conditions in the long run. Second, in Figure 5 we can see that the elastic scheme does not affect *SMR* of the entire network. It only affects *SMRs* of individual vehicles. For example, in the case of pure CSMA/CA, roughly half of the vehicles shows *SMRs* between 75-100%, while the other half shows *SMRs* between 40-75%. But, in the case of elastic scheme, this is completely changed and all vehicles show more or less the same *SMRs* that is closer to *SMR* of the entire network.

Jitter Scheme (JS): In JS, the activation time is defined as

$$a_i^{(k)} = \phi_i + kT_i + AJ_i - r(2AJ_i), \quad (24)$$

where AJ_i is an activation jitter that has a granularity of one message transmission time (i.e., $AJ = N \leftrightarrow AJ = NT_d$). The worst delays between messages of this scheme, therefore, is equal to $T_i + 2AJ_i$. Again for observations, first, similar as ES, JS improves the *fairness* and the *delay*

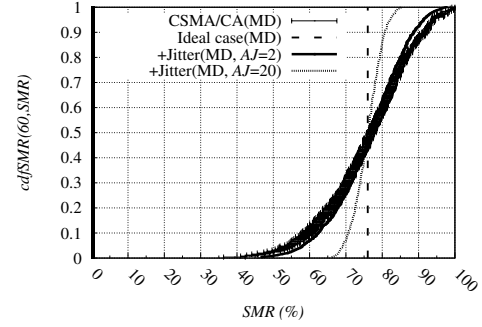
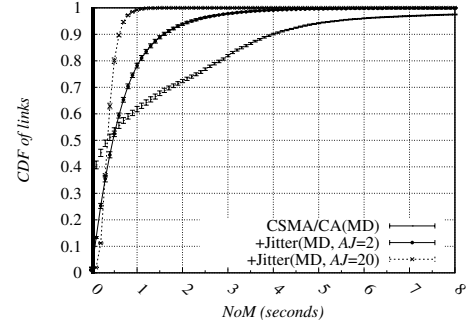
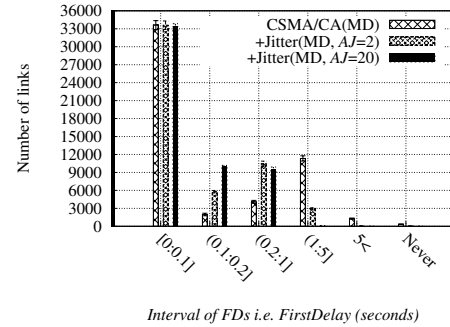

 Figure 6. ES improves the NoM significantly ($VD = 50$, $CI = 99\%$).

 Figure 7. ES improves FD significantly. When “ $er=6$ ”, the number of cases for “ $5<$ ” and “Never” are 15 ± 7 and 0, respectively while “ $er=2$ ”, these are both 0 ($VD = 50$, $CI = 99\%$).

characteristics as shown in Figure 8, 9 and 10. We chose the same AJ for all vehicles. The bigger AJ is chosen, the better JS works. Note that a small jitter size does not show much improvement. Compared to ES, JS needs a bigger jitter size to improve the fairness though a small jitter size already works pretty well on the delay characteristics. This indeed makes sense, because, in JS, the channel condition of a vehicle does not change completely compared to the ES. Let's say there are two vehicles synchronized with each other causing message collisions on their receivers. For ES, we showed that the lifetime of such synchronization becomes relatively short. But, in JS, the two vehicles would remain synchronized during their entire encounter interval. The jitter only sometimes helps to prevent the message collisions happening. In addition, we can say that JS works better than ES on the delay characteristics. Particularly, from Figure 10 we learn that the number of links on a 0.2-1s interval is much lower than that of ES.

Elastic + Jitter scheme (EJS): In addition to the previous two schemes, we also look into a third approach which is a combination of the elastic and the jitter schemes, namely EJS defined as

$$a_i^{(k)} \stackrel{\text{def}}{=} \begin{cases} \phi_i & \text{if } k = 0 \\ a1 & \text{if } k > 0, (k + \phi_e) \bmod er_i \neq 0 \\ a2 & \text{if } k > 0, k \bmod er_i = 0 \end{cases} \quad (25)$$

where $a1 = a_i^{(k-1)} + T_i + AJ_i - r(2AJ_i)$ and $a2 = a_i^{(k-1)} + r(2T_i) + AJ_i - r(2AJ_i)$, respectively. As hoped,


 Figure 8. JS can improve the fairness for bigger jitter size. ($VD = 50$, CI of 99%, for JS, $CI = \pm 1.0$)

 Figure 9. JS improves the NoM significantly. In case of $AJ=20$, 60% of the links have less than 0.5s of NoM (i.e., better than ES). ($VD = 50$, $CI = 99\%$).

 Figure 10. JS improves the FD significantly. In case of $AJ=2$, the number of cases for “ $5<$ ” and “Never” are 31 ± 6 and 29 ± 9 , respectively. In case of $AJ=20$, these are both 0 and the number of the links in an interval of (0.2:1] is much lower. ($VD = 50$, $CI = 99\%$)

this solution outperforms both previous schemes as shown in Figure 11, 13, and 12. This third solution features the advantages of both schemes. Similar as ES, it does improve the fairness drastically. Similar as JS, it improves the delay characteristics to a greater extent. .

V. CONCLUDING REMARKS

We regard the following two as the main contributions. The first is an evaluation of oPBC, where we reveal that the HN problem is the main cause of various quality degradations especially when the network is unsaturated. The detailed study shows that the (synchronized) HN causes unfair SMR distribution and long no message interval in a

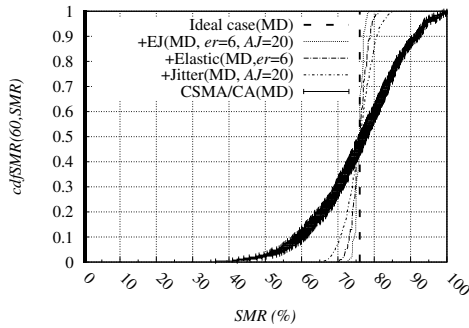


Figure 11. EJS scheme outperforms JS and it is slightly better than ES for improving the fairness (CI = ±0.3, 99%).

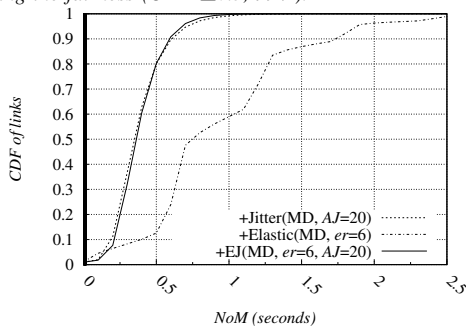


Figure 12. EJS improves the delay characteristic by reducing NoM similar as JS (VD = 50, CI = 99%).

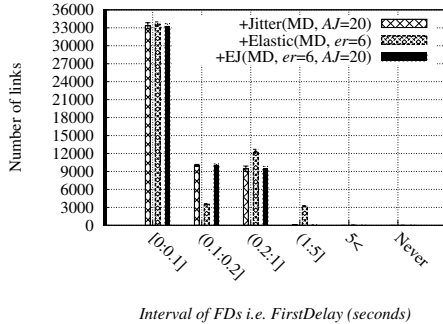


Figure 13. EJS improves the delay characteristics similar as JS (In case of EJS, the number of links for “<5” and “Never” are both 0, respectively. VD = 50, CI = 99%).

link of two vehicles. In some cases, such no message interval equals to an entire link interval. The second contribution is three simple but effective broadcasting schemes to fix the above issue that are fully compatible with the 802.11p and can be very applicable in practice. Though the three solutions do not affect the SMR (or reliability aspect) of the entire network, they do show significant improvements on the fairness and delay aspects.

REFERENCES

[1] “Final report,” Tech. Rep. DOT HS 810 591, Vehicle Safety Communications Project, 2006.
 [2] F. Bai and H. Krishnan, “Reliability Analysis of DSRC Wireless Communication for Vehicle Safety Applications,”

Intelligent Transportation Systems Conference, 2006. ITSC '06. IEEE, pp. 355–362, 2006.

[3] C. Robinson, D. Caveney, L. Caminiti, G. Baliga, K. Laberteaux, and P. Kumar, “Efficient Message Composition and Coding for Cooperative Vehicular Safety Applications,” *Vehicular Technology, IEEE Transactions on*, vol. 56, pp. 3244–3255, Nov. 2007.
 [4] J. Mittag, F. Schmidt-Eisenlohr, M. Killat, M. Torrent-Moreno, and H. Hartenstein, “MAC Layer and Scalability Aspects of Vehicular Communication Networks,” *VANET: Vehicular Applications and Inter-Networking Technologies*, pp. 219–269, 2010.
 [5] M. Torrent-Moreno, J. Mittag, P. Santi, and H. Hartenstein, “Vehicle-to-Vehicle Communication: Fair Transmit Power Control for Safety-Critical Information,” *Vehicular Technology, IEEE Transactions on*, vol. 58, pp. 3684–3703, Sept. 2009.
 [6] “IEEE Standard for Information Technology- Telecommunications and Information Exchange Between Systems-Local and Metropolitan Area Networks-Specific Requirements-Part 11: Wireless LAN Medium Access Control (MAC) and Physical Layer (PHY) Specifications,” *IEEE Std 802.11-1997*, pp. 1–445, 1997.
 [7] D. R. Choffnes and F. E. Bustamante, “An integrated mobility and traffic model for vehicular wireless networks,” *Proceedings of the 2nd ACM international workshop on Vehicular ad hoc networks*, pp. 69–78, 2005.
 [8] Q. Chen, F. Schmidt-Eisenlohr, D. Jiang, M. Torrent-Moreno, L. Delgrossi, and H. Hartenstein, “Overhaul of IEEE 802.11 modeling and simulation in NS-2,” *Proceedings of the 10th ACM Symposium on Modeling, analysis, and simulation of wireless and mobile systems*, pp. 159–168, 2007.
 [9] X. Ma and X. Chen, “Delay and Broadcast Reception Rates of Highway Safety Applications in Vehicular Ad Hoc Networks,” *2007 Mobile Networking for Vehicular Environments*, pp. 85–90, May 2007.
 [10] A. Vinel, D. Staehle, and A. Turlikov, “Study of Beaconing for Car-to-Car Communication in Vehicular Ad-Hoc Networks,” *Communications Workshops, 2009. ICC Workshops 2009. IEEE International Conference on*, pp. 1–5, 2009.
 [11] L. Yang, J. Guo, and Y. Wu, “Channel Adaptive One Hop Broadcasting for VANETs,” *Intelligent Transportation Systems, 2008. ITSC 2008. 11th International IEEE Conference on*, pp. 369–374, 2008.

Efficient Adaptive Equalizer Combined with LDPC Code for Vehicular Communications

Do-Hoon Kim, Junyeong Bok and Heung-Gyoon Ryu

Department of Electronic Engineering

Chungbuk National University

Cheongju, Korea

neon86@nate.com, bjiy84@nate.com, ecomm@cbu.ac.kr

Abstract—Low density parity check (LDPC) code is very powerful for the error correction in the communication systems. So, LDPC code has been adopted for the standard of IEEE 802.11p (vehicular ad-hoc networks) and digital video broadcasting-satellite2 (DVB-S2). Features of LDPC code are iterative decoding and sparse parity check matrix. However, when multipath fading channel is considered, LDPC code needs long parity check matrix and pretty big iteration number of decoding. We propose a fast and efficient adaptive equalizer with LDPC code for compensating the carrier frequency offset (CFO) and phase noise in the vehicular environments. In addition, this proposed system has less iterations than the conventional system without combining structure. So, the proposed system has lower complexity. In this paper, we investigate the system model and evaluate BER performance for the vehicular environments by the simulation results, considering the CFO and phase noise in the OFDM system.

Keywords—LDPC; adaptive equalizer; CFO; phase noise; OFDM; Sparse Parity Check Matrix; iteration number.

I. INTRODUCTION

There are some impairments degrading the OFDM communication system. One is phase noise caused by the oscillator in transceiver; another is CFO (carrier frequency offset). These components produce the ICI (inter-subcarrier interference). Until now, in fact, there are many methods to compensate CFO [1]-[2] or phase noise [3]-[5] in OFDM system. Therefore, we can overcome ICI effect by using forward error correction code and equalization in OFDM system [6]-[12].

Especially, LDPC code is well known as the good performance channel coding method. LDPC code was firstly proposed by Robert G. Gallager in 1962 [13] and re-considered by Mackay and Neal in 1997 [14] [15]. LDPC is the error correction code which shows the closest performance to Shannon's limit [14]. Recently, LDPC code has been commonly used in such as Mobile WiMax and DVB-S2. LDPC code has highly error correction performance at low Signal to Noise Ratio (SNR) environment and is able to encode fast by using sparse parity check matrix. However, when multipath fading channel is considered, LDPC code needs long sparse parity check matrix and iteration number of decoding.

In this paper, we propose an adaptive equalizer combined with LDPC code. The proposed system requires a smaller

iteration number of LDPC decoding than the system without combining. In addition, this combined adaptive equalizer can compensate ICI effect which degrades the BER performance, such as CFO and expand ICI in OFDM system[1]-[5]. So, we consider about CFO and phase noise effects in OFDM system. At first, we analyze the basic principle of LDPC code and frequency domain equalizer [6]-[12]. After that, we evaluate BER performance of the combined adaptive equalizer for vehicular environments.

II. SYSTEM MODEL

Fig. 1 shows the system model of the combined adaptive equalizer with LDPC code in OFDM system [6]. We use LDPC code and channel estimator to estimate channel characteristic in OFDM communication system. It can eliminate ISI (inter-symbol interference) effects by using CP (cyclic prefix). Then, it can estimate the channel characteristic through the long preamble and equalize the channel fading. Especially, we design and propose a feedback loop composed up of LDPC decoder to adaptive equalizer. That is, adaptive equalizer is combined with LDPC decoder iteratively. The combined equalizer calculates the control factor in feedback loop iteratively. So, we can call adaptive equalizer combined with LDPC code.

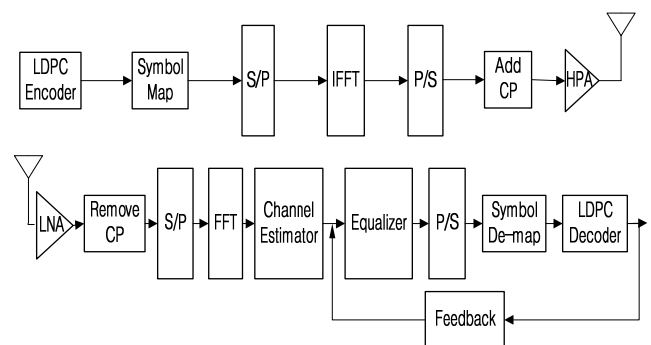


Figure 1. System model of the adaptive equalizer.

III. LOW DENSITY PARITY CHECK CODE

LDPC code is one of the block coding methods. It can be expressed as (N, K) . It has a sparse parity check matrix (H

matrix) of $(N - K) \times N$ size. H matrix is non-systematic sparse parity check matrix.

A. LDPC Encoding

The received vector is corrupted by an error vector \mathbf{e} as follows [16].

$$\mathbf{r} = \mathbf{c} \oplus \mathbf{e} = [\mathbf{p} \quad \mathbf{m}] \oplus \mathbf{e}, \quad (1)$$

where \mathbf{p} is parity vector and \mathbf{m} is message vector. The parity vector and message vector are assumed to be located at the former or latter part of the code vector, respectively. The decoder of the receiver is supposed to apply for the received signal vector to find the syndrome vector as [16]:

$$\begin{aligned} \mathbf{s} = \mathbf{r}H^T &= ([\mathbf{p} \quad \mathbf{m}] \oplus \mathbf{e}) \begin{bmatrix} H_1^T \\ H_2^T \end{bmatrix}. \\ &= \mathbf{p}H_1^T \oplus \mathbf{m}H_2^T \oplus \mathbf{e}H^T \end{aligned} \quad (2)$$

Noting that this syndrome vector should be zero for the non-error case, that is, $\mathbf{e} = \mathbf{0}$.

$$\mathbf{s} = \mathbf{p}H_1^T \oplus \mathbf{m}H_2^T = \mathbf{0}. \quad (3)$$

We can write the parity vector \mathbf{p} in terms of the message vector \mathbf{m} as [16]

$$\mathbf{p} = \mathbf{m}H_2^T H_1^{-T}. \quad (4)$$

This amounts to the generator matrix

$$G = [H_2^T H_1^{-T} \quad I], \quad (5)$$

so the code vector can be generated by post-multiplying the message vector \mathbf{m} with the generator matrix G as [16]

$$\mathbf{c} = \mathbf{m}G = [\mathbf{m}H_2^T H_1^{-T} \quad \mathbf{m}] = [\mathbf{p} \quad \mathbf{m}]. \quad (6)$$

B. LDPC Decoding

The LDPC decoder calculates the probability in variable nodes and check nodes, respectively [17] [18]. Decoding algorithms can be divided into sum-product (SP) algorithm and min-sum (MS) algorithm. SP algorithm has better decoding performance, but higher complexity. So, we choose SP algorithm to decode because of decoding performance. The LDPC decoder operates through 4 steps. First step is the initializing step. Second step is the updating check nodes step. Third step is the updating variable nodes step. Final step is decision step.

IV. CHANNEL ESTIMATION AND EQUALIZATION

A frequency-domain training sequence is

$$X(k) = X_R(k) + jX_I(k) \quad (7)$$

with the corresponding channel output.

$$Y(k) = Y_R(k) + jY_I(k). \quad (8)$$

Channel estimation with $X(k)$ and $Y(k)$ is

$$H_p = \frac{Y(k)}{X(k)} \quad (9)$$

The long preamble used for channel estimation is

$$X(k) = 1 \quad \text{or} \quad -1 \quad (\text{with} \quad X_I(k) = 0) \quad (10)$$

The channel estimation signal can be simplified as

$$H_p = \frac{Y(k)}{X(k)} = \frac{Y_R(k) + jY_I(k)}{X_R(k)} \quad (11)$$

Since the long preamble contains two repeated training sequences, the average of the FFT ($Y_1(k)$ and $Y_2(k)$) of the channel outputs can be taken for the better channel estimation.

$$H_p = \frac{1}{2} \frac{Y_1(k) + Y_2(k)}{X(k)} \quad (12)$$

So, the estimated channel can equalize the output to compensate the channel effect.

$$\hat{X}(k) = \frac{Y'}{\hat{H}_p} \quad (13)$$

V. PROPOSED ADAPTIVE EQUALIZER COMBINED WITH LDPC CODE

Fig. 2 shows the feedback system of the combined adaptive equalizer in the receiver side. Fig. 2 shows subsystem after FFT operation in OFDM receiver side. Original equalization type is the zero forcing, but the combined equalizer with LDPC decoder is almost same to the decision feedback equalizer because it performs feedback loop between equalizer and LDPC decoder iteratively. So, we call as adaptive equalizer combined with LDPC code.

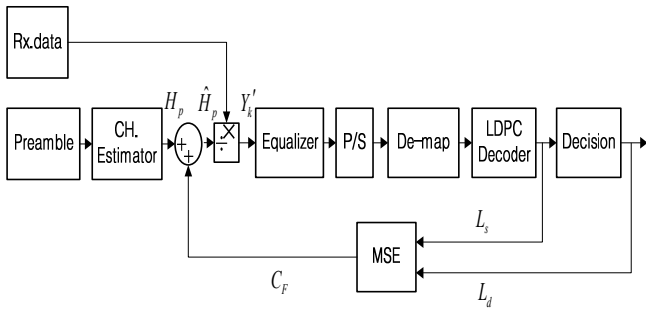


Figure 2. Block diagram of combined adaptive equalizer in receiver.

As shown in Fig. 2, after through LDPC decoder, the proposed system feeds C_F back to adaptive equalizer from LDPC decoder to compensate channel estimation with L_s and L_d . L_s and L_d are decoder output and decision bit, respectively.

$$\tilde{L}_s = \text{norm}(L_s) \quad (14)$$

$$\hat{L}_k = \sum_{k \in s_d} \tilde{L}_s^* L_d \quad (15)$$

$$C_F = \frac{\hat{L}_k}{\sum_{k \in s_d} |\tilde{L}_s|^2} \quad (16)$$

\hat{H}_p is the channel characteristic after estimation by the long preamble adding C_F .

$$\hat{H}_p = H_p + C_F \quad (17)$$

We can improve performance by the following equation with compensated channel \hat{H}_p .

$$Y'_k = \frac{Y_k}{\hat{H}_p} \quad (18)$$

Therefore, the combined adaptive equalizer can achieve better performance like the decision feedback equalizer. Basically, equalization type is based on the zero forcing, but the combined adaptive equalizer with LDPC decoder is almost same to the decision feedback equalizer because of feedback loop between equalizer and LDPC decoder.

VI. SIMULATION RESULTS

Table 1 shows simulation parameters for the combined adaptive equalizer with LDPC code. In this paper, we consider IEEE 802.11p format. Code rate is 3/4 and parity check matrix size is 720. At first, we generate 78 bits per data block. We change block size to 540 bits through the buffer and encode as 720 bits. Then, we change again to 104 bits in order to modulate through the buffer. Finally, we can output as 52 data symbols. We consider the AWGN and multipath channel. The multipath channel considers the ITU vehicular channel model. Furthermore, we adapt the normalized CFO and phase noise power as 0.03 and -12dBc, respectively.

TABLE I. SIMULATION PARAMETERS.

Parameters	Values
# of data subcarriers	52
# of pilot subcarriers	4
# of padded zeros	7
FFT size	64
# of samples in a GI	16
Modulation level	4QAM
Multipath channel	ITU vehicular channel A

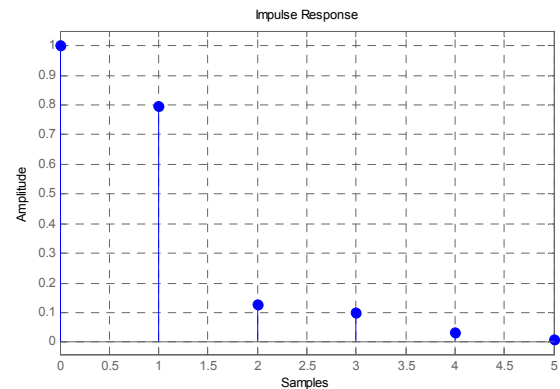


Figure 3. Impulse response of considered multipath channel.

Fig. 3 shows the impulse response of the considered multipath channel. This multipath channel is called as ITU-Vehicular channel A. The multipath channel can be simplified in the digital FIR filter model. Overall 5 delay paths may exist.

Fig. 4 shows BER curve according to iteration number of the LDPC decoding in AWGN channel. The iterations is higher, BER performance can be improved.

Fig. 5 shows BER performance of the combined adaptive equalizer and without channel estimation and equalization. The combined adaptive equalizer has much better performance than without channel estimation and equalization over considered CFO and phase noise effects. When iteration number is 5, the SNR is less than 5dB at 10^{-5} error probability. So, the combined adaptive equalizer is able to compensate the CFO and phase noise.

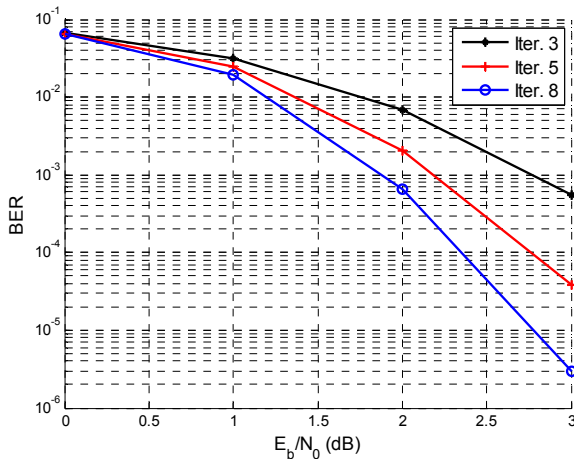


Figure 4. BER performance according to iteration number in AWGN.

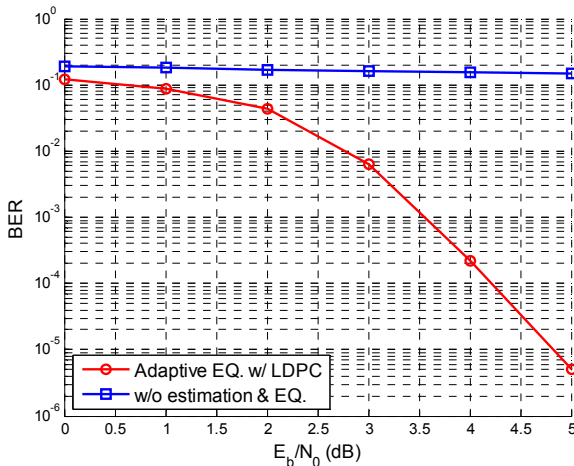


Figure 5. Comparison BER performance of the combined adaptive equalizer and BER without channel estimation and equalization.

Fig. 6 shows BER performance of the combined adaptive equalizer and without combining system under same iteration number situation. Performance of the combined adaptive equalizer is better than without combining system. The combined adaptive equalizer is better performance about 0.5dB at 10^{-4} when iteration number is 5.

Fig. 7 shows closely similar BER performance between the combined adaptive equalizer and without combining system at same iterations. When SNR is 3.5dB, BER of the combined adaptive equalizer and without combining system is exactly same. Where, iteration number of the combined adaptive equalizer is 3, but without combining system is 5. Because complexity of system is closely related to iteration number, the combined adaptive equalizer has lower complexity than without combining system.

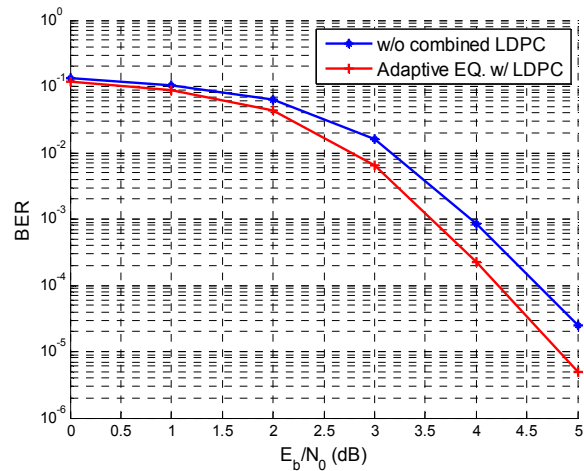


Figure 6. BER performance of the combined adaptive equalizer and BER without combining.

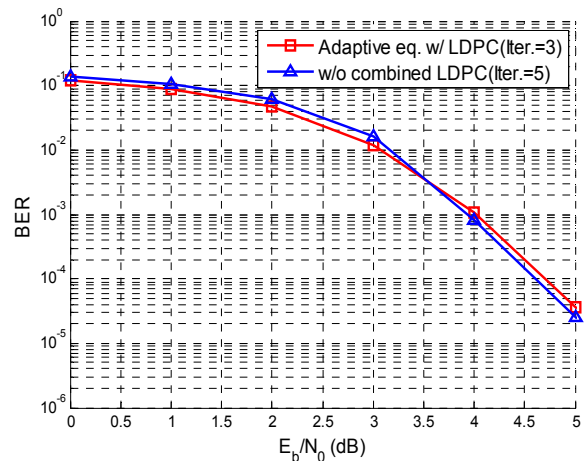


Figure 7. Comparison BER performance of adaptive equalizer combined with LDPC and BER without combining.

VII. CONCLUSION

We propose an efficient adaptive equalizer combined with LDPC code to compensate the CFO and phase noise in vehicular environments. To estimate the channel, combined adaptive equalizer uses the long preamble. After passing through the LDPC decoder, the proposed system calculates C_F with L_s and L_d . Then, it feeds C_F back into the equalizer from the LDPC decoder. So, BER performance of the combined adaptive equalizer can be improved. On the other hands, the combined adaptive equalizer can achieve lower complexity when it has same performance. The combined adaptive equalizer has good BER performance with CFO and phase noise. As a result of Fig. 5, the combined adaptive equalizer shows better BER performance than without combining. Also, as a result of Fig. 6, iteration number of combined adaptive equalizer is lower than the system without combining when both of performances are closely similar. That is, complexity is lower than the system without combining

because complexity is related to iterations of the LDPC decoder. So, the combined adaptive equalizer can compensate CFO and phase noise through combining in OFDM system. Therefore, it can improve BER performance and reduce complexity of the LDPC decoder. Additionally, we can expect implementation of the combined adaptive equalizer for vehicular communications.

ACKNOWLEDGEMENT

This research was supported by Basic Science Research Program through the National Research Foundation of Korea(NRF) funded by the Ministry of Education, Science and Technology(No. 2010-0007567).

REFERENCES

- [1] P. H. Moose, "A technique for OFDM Frequency Offset Correction," *IEEE Trans. on Comm.*, vol. 42, no. 10, pp. 2908-2914, 1994.
- [2] T. Pollet, M van Bladel, M. Moeneclaey, "BER sensitivity of OFDM systems to carrier frequency offset and Wiener phase noise," *IEEE Trans. On Comm.*, vol. 43, no. 2, pp. 887-895, 1995.
- [3] Gholami, M. R., Nader-Esfahani, S., Eftekhar, A. A., "A new method of phase noise compensation in OFDM." *ICC '03. IEEE International Conference on Communications*, vol. 5, pp. 3443-3446, 2003.
- [4] Songping Wu, Bar-Ness. Y., "A phase noise suppression algorithm for OFDM-based WLANs," *IEEE Communications Letters*, vol. 6, pp. 535-537, 2002.
- [5] H. G. Ryu, Y. S. Li., "Phase noise analysis of the OFDM communication system by the standard frequency deviation." *IEEE Transactions on Consumer Electronics*, vol. 49, no. 1, pp. 41-47, 2003.
- [6] SHAHID U. H. QURESHI, "Adaptive Equalization," *PROCEEDINGS OF THE IEEE*, VOL. 73. NO. 9, Sep. 1985.
- [7] Z.-S. Lin, T.-L. Hong and D.-C. Chang, "Design of an OFDM system with long frame by the decision-aided channel tracking technique". *Proc. IEEE Sixth Electro/Information Technology Conf.*, Lansing, MI, USA, May 2006.
- [8] S. Kalyani, and K. Giridhar, "Quantised decision based gradient descent algorithm for fast fading OFDM channels". *Proc. IEEE 60th Vehicular Technology Conf.*, September 2004, pp. 534-537.
- [9] R. Funada, H. Harada, and S. Shinoda, "Performance improvement of decision-directed channel estimation for DPC-OF/TDMA in a fast fading environment". *Proc. IEEE 60th Vehicular Technology Conf.*, September 2004, pp. 5125-5129.
- [10] H.-W. Kim, C.-H. Lim, and D.-S. Han, "Viterbi-decoder aided equalization and sampling clock track of OFDM WLAN". *Proc. IEEE 60th Vehicular Technology Conf.*, September 2004, pp. 3738-3742.
- [11] Q. Yuan, C. He, K. Ding, W. Bai, and Z. Bu, "Channel estimation and equalization for OFDM system with fast fading channels". *Proc. IEEE 60th Vehicular Technology Conf.*, September 2004, pp. 452-455
- [12] T. Kella, "Decision-directed channel estimation for supporting higher terminal velocities in OFDM based WLANs". *Proc. IEEE Global Telecommunication Conf.*, December 2003, pp. 1306-1310.
- [13] R. G. Gallager, "Low Density Parity Check codes," *IRT Trans. Inform. Theory*, vol. IT-8, pp. 21-28, Jan. 1962.
- [14] D. J. Mackay and R. M. Neal, "Neal Shannon limit performance of low density parity check codes," *Electronic letters*, vol. 45, pp. 457-458, March 1997.
- [15] D. J. Mackay, "Good error correcting codes based on very sparse matrix," *IEEE Trans. Inform. Theory*, vol. 33, no. 6, pp. 399-431, March 1999.
- [16] W. Y. Yang, "MATLAB/Simulink for Digital Communication," A-Jin, 1st ed, pp. 309-313.
- [17] S. Papaharalabos, P. Sweeney, B. G. Evans, P. T. Mathiopoulos, G. Albertazzi, A. Vanelli-Coralli and G. E. Corazza, "Modified sum-product algorithms for decoding low-density parity-check codes," *IET Commun.*, vol. 1, pp 294-300, June 2007.
- [18] S. L. Howard, Christian Schlegel and V. C. Gaudet, "A degree-matched check nod approximation for LDPC decoding," *Proc. IEEE Int. symp. Inf. Theory(ISIT)*, Adelaide, Australia, pp. 1131-1135, Sep. 2005.

Intelligent Traffic Control Based on Multi-armed Bandit and Wireless Scheduling Techniques

Chanwoo Park and Jungwoo Lee

School of Electrical Engineering and Computer Sciences

Seoul National University, Seoul 151-744, Korea

Email: cpark@wspl.snu.ac.kr and junglee@snu.ac.kr

Abstract—Intelligent Transportation System (ITS) researches, including vehicular communications, have been making great advancements to improve road safety and traffic flow efficiency. In this paper, we propose two new traffic control systems. In the first method, we assume a system with fully autonomous cars and infrastructure to avoid collision completely. Vehicles communicate with the access point in both random access mode and polling mode, and the movement of the automobiles will be coordinated by the infrastructure using IEEE 802.11 DCF/PCF mechanisms. In the second method, there is a given set of lanes with unknown reward statistics and we consider the lanes as a multi-armed bandit. We use multi-armed bandit algorithm to choose the best lane to drive in and to maximize the total expected reward while minimizing the regret. Traffic congestion is very difficult to predict and deal with because it is a function of many unknown factors such as number of cars, weather, road constructions, and accidents. The proposed algorithms are designed for urban road networks to ease the congestion, and make it more predictable at the same time. We find that the first algorithm makes the traffic system able to balance efficiency and fairness and the second algorithm helps vehicles choose the best lane with minimized regret.

Keywords—ITS; Vehicular Network; IEEE 802.11 DCF/PCF; MAB.

I. INTRODUCTION

Driverless cars are vehicles with fully automated driving capabilities [1]. In many urban environments, a rapid increase in the number of cars has caused severe problems such as traffic congestion, air pollution and road safety. Researchers have been putting a lot of effort into developing new types of transportation systems (e.g., driverless cars) as a solution to this problem. Researchers first pondered the idea of driverless cars in the 1970s [2]. Since then, there have been many prototypes of driverless cars tested and lots of research and development on driverless cars going on. VisLab (Artificial Vision and Intelligent Systems Laboratory) has successfully completed the rally of 13,000 km from Milan to Shanghai on driverless vehicles in 2010. There has been active research on vehicle network going on to develop interactive system enabling a number of new services for road safety, mobility and efficiency such as Vehicle Infrastructure Integration (VII) [3] and the California Partners for Advanced Transit and Highways (PATH) [4].

In many cities, especially in large metropolises, traffic congestion during rush-hours is one of major problems. Traffic congestion is a very tricky problem to deal with not only

because it makes trip times longer and increase vehicular queuing but also because there are too many variables on road networks, such as number of cars at a certain time, weather of that day, unexpected road construction and car accidents etc. Because of this uncertainty of road networks, it is very difficult to predict and deal with the traffic congestion properly.

There are two basic assumptions in this paper. First, vehicles are fully self-driven, which means each vehicle knows its destination and drives from one place to another without input from a human operator. Secondly, we assume that the system is established to completely avoid collisions between cars. This central system manages the car network to make the road environment collision-free.

Based on these assumptions, we propose an algorithm which is used for traffic control when there is no traffic light at intersections. The basic principle of this algorithm is that the system gives priority to the lane which has the longer queue of cars so that more congested lanes can be relieved more quickly. This will make travel times during rush-hour more predictable. There are two values we have to consider when it comes to traffic control without traffic lights, which are flow efficiency and fairness between users. The proposed algorithm in this paper uses IEEE 802.11 DCF/PCF Mechanisms to balance these two values.

The rest of this paper is organized as follows: Section II introduces the proposed system using IEEE 802.11 legacy DCF/PCF and its performance. After describing the second proposed system which is based on multi-armed bandit algorithm in Section III, the paper concludes with Section IV.

II. TRAFFIC CONTROL BASED ON IEEE 802.11 DCF/PCF MECHANISMS

The system algorithm and the system model are introduced.

A. IEEE 802.11 legacy DCF/PCF

The IEEE 802.11 standard makes it mandatory for all stations to implement the Distributed Coordination Function (DCF), a form of Carrier Sense Multiple Access with Collision Avoidance (CSMA/CA) [5]. CSMA is a contention-based protocol which makes sure that all stations first sense the medium before transmitting. The main goal is not to have stations transmitting at the same time, which results in collisions and corresponding retransmissions. Probabilistically speaking, they have the same opportunities when stations contending for

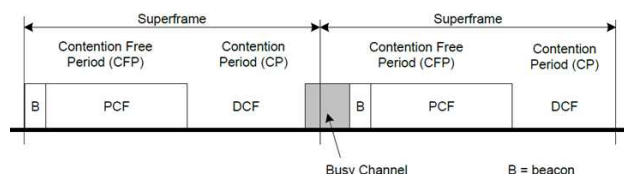


Fig. 1. IEEE 802.11 legacy DCF/PCF operation between beacon intervals

medium access in DCF mode. Each station has its own random back off timer when contending so they can achieve fairness in the long-term.

There is another optional access method, namely, the point coordination function (PCF) based on poll-and-response mechanism. PCF is intended to transmit real-time information such as VoIP, streaming video. In PCF mode, a point coordinator within the Access Point (AP) controls which stations can transmit during a certain given period of time, which is called the Contention Free Period (CFP). The point coordinator will take a look through all stations which are operating in PCF mode and poll them one at a time. Therefore, PCF is a contention-free protocol enabling stations to transmit data frames continuously.

AP sends beacon frames at regular intervals so that the IEEE 802.11 protocol makes stations alternate between the use of DCF and PCF in a single interval. With DCF, stations will compete for the channel access by using CSMA. For the following CFP, the stations will wait for a poll from the point coordinator before sending data frames as shown in Fig. 1. Therefore, DCF is basically a protocol based on random contention so it aims for fairness while PCF is a protocol controlled by the point coordinator trying to give opportunities to stations which need to be served first. In the following section, we discuss how we can apply this IEEE 802.11 DCF/PCF mechanism to traffic control system.

B. System Model

There is a four-way intersection and each road has eight lanes. In the i th lane, cars are generated by Poisson distribution with expected number (arrival rate) λ_i every time slot. This system assumes that all cars are driverless and safely controlled by the car network system so that collision avoidance system is perfectly implemented. In each direction, the first lane is dedicated for left-turns, the second and third lanes are for cars going straight and the fourth lane is only for right-turns. This is described in Fig. 2.

1) *Contention-Free Period (CFP)*: The system divides each repeat interval into two parts, Contention Period and Contention-Free Period just like IEEE 802.11 DCF/PCF. In Contention-Free Period, we have total sixteen lanes as incoming channel to the intersection and each lane has its own fixed route to pass through the intersection. Some of the routes can overlap each other; so, traffic control is needed on the overlapping spot. Let Q_i denote the number of cars queued up before entering the intersection in the i th lane ($i = 1, \dots, 16$) and Q_i is updated at the very beginning of each time slot.

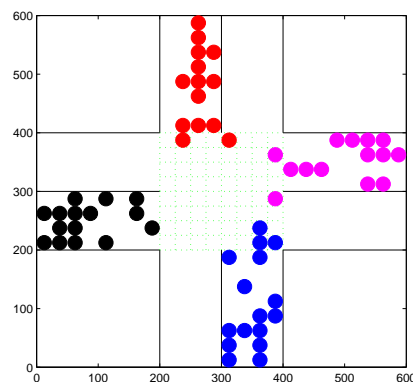


Fig. 2. Basic simulation model

When the i th route and the j th route intersect and there are two cars, one from i th lane and another one from the j th lane, going to the intersecting point, the system has to decide which car it will let go first. The decision will be made based on which one is larger between Q_i and Q_j . If there are n lanes (x_1, \dots, x_n) whose routes crossing each other, the system will give priority to the x th lane, which satisfies,

$$x = \arg \max_{i \in x_1, \dots, x_n} Q_i \quad (1)$$

2) *Contention Period (CP)*: If the system always give priority to the most congested lane, the car on the road which is relatively free of traffic will have to wait until its lane become the most congested. It is not fair to force the cars on the less congested lane to wait for too long just because the other lane is very busy. This motivates us to introduce contention period. In CP, if there are n cars coming to the overlapping spot at the same time, the n cars will take turns to pass through the overlapping spot no matter how many cars are queuing up in each lane. When you design a system you can make CFP longer if your main goal is to ease the congestion, or you can make CP longer if you aim for fairness. The proposed traffic control system with/without traffic light are shown in Fig. 3 and Fig. 4, respectively.

C. Simulation Results

1) *Proposed traffic system vs. Traditional traffic system* : Now we compare the proposed traffic system with traditional traffic system which are characterized by the existence of traffic lights. We put different weight on each lane with different Poisson expectation, i.e. $\lambda_{North} = 1/2$, $\lambda_{South} = 1/4$, $\lambda_{East} = 1/8$, $\lambda_{West} = 1/16$, so that each lane has different level of congestion. We measure the travel time for a car to pass through the intersection. One cycle (repeat interval) of the system consists 60 time slots with 30 time slots of CFP and 30 time slots of CP. The result is shown in Table I.

When the proposed system is used, the elapsed time of a single car to pass through the intersection is reduced by 34.4 % on average, which means total traffic flow become smoother.

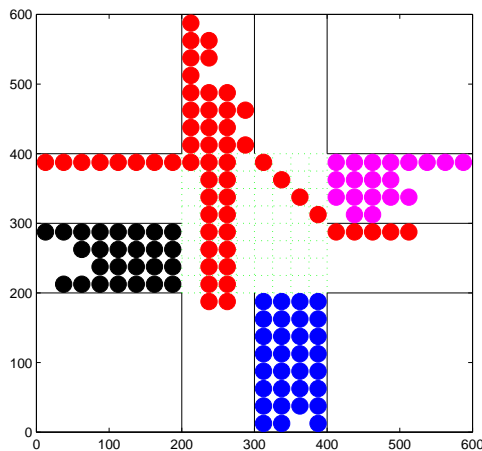


Fig. 3. Traditional traffic system with traffic lights

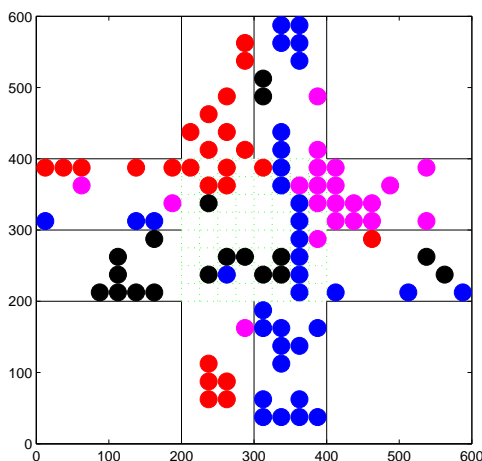


Fig. 4. Proposed traffic system without traffic lights

Another notable result is that variance between travel times of different users is significantly decreased by 90.5 %. This reduced variance means that the travel time become much more predictable even though each road has different traffic density. Fig. 5 shows this result in Gaussian distribution. We can confirm that the travel time for each user become shorter and a lot more predictable by using the proposed traffic system.

2) *Traffic density and the system performance:* Now we analyze the relationship between the traffic density and the system performance. We can expect by intuition that the proposed system will work more efficiently if there is less traffic on the road. For example, there are probably few cars on the road during late nights or early dawns, which means they need not wait before entering the intersection. In this simulation, we measure the travel time as a function of traffic density. As you can see in Fig. 6, the travel time in the proposed system barely increase until traffic density reaches

TABLE I
TRAVEL TIME WITH/WITHOUT TRAFFIC LIGHT

(unit: time slot)	Traditional system (with traffic light)		Proposed system (without traffic light)	
	Variance ($\times 10^4$)	Average ($\times 10^2$)	Variance ($\times 10^4$)	Average ($\times 10^2$)
Left turn	36.85	11.23	0.78	4.05
Straight	145.2	22.43	12.74	16.09
Right turn	36.44	11.20	4.53	9.30

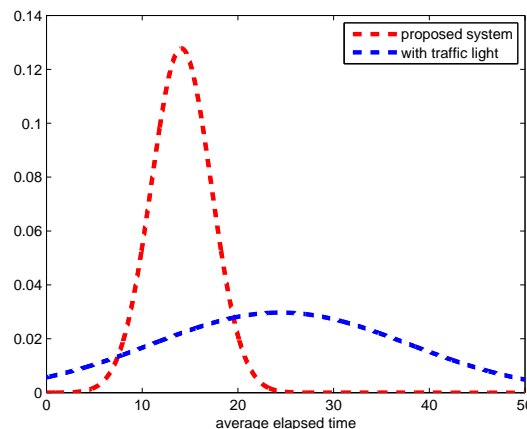


Fig. 5. Gaussian distribution model of travel time

a certain number, 0.2 cars per time slot in this graph. That means road capacity in the proposed system is able to let cars pass through the intersection without stoppage until the traffic density reaches 0.2 cars per time slot. After the traffic density of 0.2, the travel time in the proposed system starts to increase almost linearly. After applying linear estimation we find the slope of estimated line, and it is shown in Table II. Even traffic density become higher than 0.2, the slope of the travel time with respect to traffic density in the proposed system is still lower than traditional system.

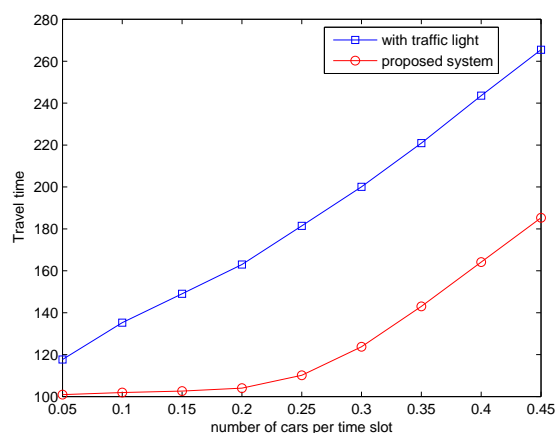


Fig. 6. Relationship between traffic density and travel time

TABLE II
 SLOPE OF TRAVEL TIME ACCORDING TO TRAFFIC DENSITY

	With traffic light	Proposed system	note
Left turn	21.7	16.8	22.6% reduced
Straight	43.3	27.8	35.8% reduced

3) *Efficiency vs. Fairness*: The proposed algorithm is based on CFP/CP of the IEEE 802.11 DCF/PCF mechanisms. The proportion of CFP and CP can be adapted according to the degree of traffic congestion. The longer CFP the system has, the more efficient the system becomes so that it can ease the traffic congestion faster. On the other hand, the longer CP ensures fairness between users, which means the users on the less congested road do not have to suffer for the sake of overall system efficiency. In our simulation, we set a repeat interval to be 60 time slots and divide the repeat interval into CFP/CP. In Fig. 7, we plot the variance of the travel time as we increase the proportion of CFP to CP. The graph shows that the higher proportion of CFP in the repeat interval makes variance of the travel time smaller, so the travel time becomes more predictable as we expected.

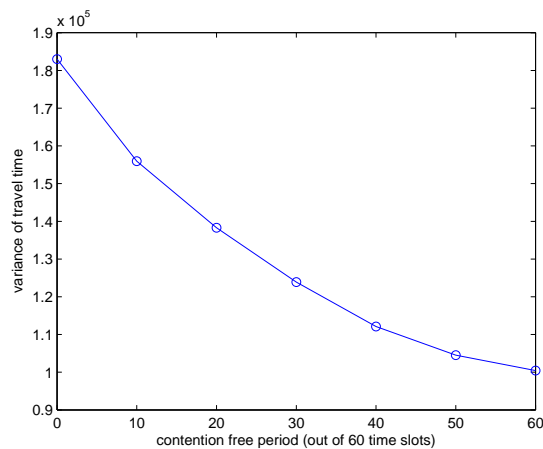


Fig. 7. Contention free period vs. variance of travel time

III. TRAFFIC CONTROL BASED ON MULTI-ARMED BANDIT ALGORITHM

A. Multi-armed bandit Policy

Multi-armed bandit (MAB) problems are a class of sequential resource allocation problems concerned with allocating one or more resources among several alternative projects. Such problems are paradigms of a fundamental conflict between making decisions that yield high current rewards, versus making decisions that sacrifice current gains with the prospect of better future rewards [6]. A policy is an algorithm that chooses the next machine to play based on the sequence of past plays and obtained rewards. Let $T_i(n)$ be the number of times machine i has been played during the first n plays. Then the regret of a certain policy after n plays is defined by

$$\mu^* n - \mu_j \sum_{j=1}^K E[T_j(n)] \quad \text{where } \mu^* = \max_{1 \leq i \leq K} \mu_i \quad (2)$$

and $E[\cdot]$ denotes expectation. Thus, the regret is the expected loss due to the fact that the policy does not always play the best machine [7].

B. System Model

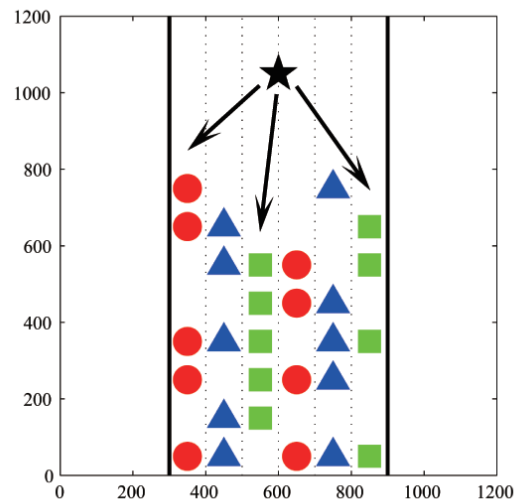


Fig. 8. Lane Selection Algorithm using MAB

We have a road with 6 lanes and each lane is randomly congested according to a given distribution as shown in Fig. 8. If a vehicle can move forward within a certain time period because there is no traffic congestion, we consider that the vehicle receives a *reward*. The vehicle chooses one lane to drive in and obtains a reward drawn i.i.d. over time from a distribution with unknown mean. Different lanes may have different reward distributions. The objective of the proposed algorithm is to find a policy that maximizes the total expected reward and to converge to the best lane while minimizing the regret.

Upper Confidence Bound (UCB) algorithm is used in this simulation as a sequential lane selection policy. The vehicle will drive in lane i that maximizes the priority index below,

$$\text{Priority}_i = \bar{x}_i + \sqrt{\frac{2 \ln n}{n_i}} \quad (3)$$

where \bar{x}_i is the average reward obtained from lane i , n_i is the number of times lane i has been played so far, and n is the overall number of plays done so far.

C. Simulation Results

We have four lanes to choose from in the simulation and each lane has its own reward distribution, $R_i = \{0.1, 0.3, 0.5, 0.7\}$, where R_i means the probability that a

vehicle can move forward without being stuck in traffic. The goal of this simulation is to find the best lane while minimizing the regret. In the simulation, policy UCB performs better than policy ϵ -GREEDY, as it is shown in Fig. 9. We can see that the lane a vehicle chooses and drives in converges to the best lane more quickly when it is played by policy UCB. The regret of policy UCB is also less than policy ϵ -GREEDY.

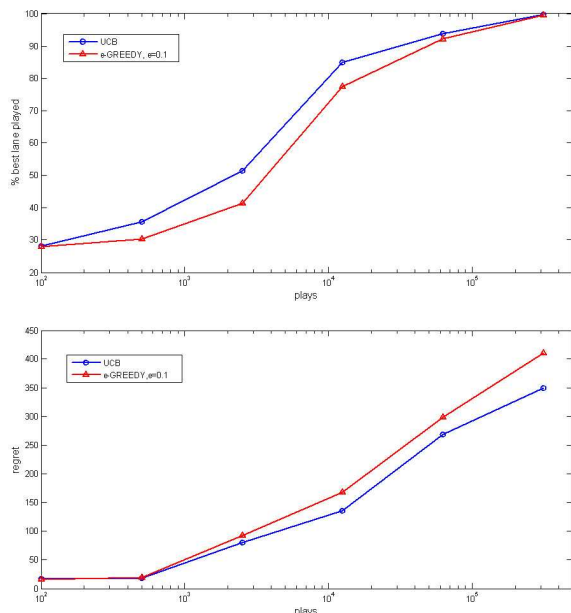


Fig. 9. Performance of different lane selection policies

IV. CONCLUSION

With the advent of driverless car technologies, a new intelligent transport system can be developed to make traffic system more efficient and safe with the help of vehicle-to-vehicle and vehicle-to-infrastructure communications. As part of this intelligent system, we have introduced a new traffic system model specifically designed for urban road networks. The proposed system based on wireless scheduling technique has no traffic lights at intersections, and uses IEEE 802.11 DCF/PCF mechanisms to control the traffic especially during rush hours. Each cycle of traffic control is divided into contention free period (CFP) and contention period (CP). In CFP, the system will try to clear up the most congested lane while the system will address the fairness issue in CP. We can achieve a proper balance between efficiency of the system and user fairness by using the proposed algorithm. The proposed algorithm can easily accommodate emergency traffic by giving the highest priority to emergency vehicle such as police cars, fire trucks, and ambulances. In the second proposed system, we utilize multi-armed bandit algorithm to tackle the lane selection problem when a vehicle faces exploration vs. exploitation dilemma. We apply UCB algorithm to the traffic system for maximization of the total expected reward. Other advanced policies for MAB problems can also be employed.

It appears that the proposed traffic control system is promising to alleviate traffic congestion in urban road systems.

ACKNOWLEDGMENT

This research was supported in part by Basic Science Research Program (2010-0013397) and Mid-career Researcher Program (2010-0027155) through the National Research Foundation of Korea (NRF) funded by the Ministry of Education, Science and Technology, Seoul R&BD Program (JP091007, 0423-20090051), Power Generation & Electricity Delivery of the KETEP grant funded by the Korea government Ministry of Knowledge Economy (No. 2011T100100151), the Institute of New Media & Communications (INMAC), and the BK21 program.

REFERENCES

- [1] R. Benenson, S. Petti, T. Fraichard, and M. Parent, "Towards urban driverless vehicles," *International Journal of Vehicle Autonomous Systems*, Volume 6, Number 1-2, pp.4-23, 2008
- [2] S. Tsugawa, T. Yatabe, T. Hirose, and S. Matsumoto, An automobile with artificial intelligence, in Proc. IJCAI, pp. 893-895, 1979
- [3] S.E. Shladover, *Preparing the Way for Vehicle-Infrastructure Integration*, California. Dept. of Transportation, 2005
- [4] J.A. Misener and S.E. Shladover, "PATH investigations in vehicle-roadside cooperation and safety: a foundation for safety and vehicle-infrastructure integration Research," *IEEE ITSC*, 2006
- [5] IEEE Std. 802.11-1999, Part 11: Wireless LAN Medium Access Control (MAC) and Physical Layer (PHY) specifications, Reference number ISO/IEC 8802- 11:1999(E), IEEE Std. 802.11, 1999 edition, 1999
- [6] A. Mahajan and D. Teneketzis, "MULTI-ARMED BANDIT PROBLEMS," in *Foundations and Applications of Sensor Management*, pp. 121-151, Springer-Verlag, 2007
- [7] P. Auer, N. Cesa-Bianchi, and P. Fischer, "Finite time analysis of the multiarmed bandit problem," *Machine Learning*, Volume 47, pp.235-256, 2002